Received: 21 September 2017 | Revised: 17 January 2018 | Accepted: 8 February 2018

DOI: 10.1002/joc.5491

International Journal of Climatology RMetS

RESEARCH ARTICLE

Development of a time-varying downscaling model considering non-stationarity using a Bayesian approach

Subbarao Pichuka | Rajib Maity

Department of Civil Engineering, Indian Institute of Technology Kharagpur, Kharagpur, India

Correspondence
R. Maity, Department of Civil Engineering, Indian Institute of Technology Kharagpur, Kharagpur 721302, West Bengal, India.
Email: rajib@civil.iitkgp.ernet.in; rajibmaity@gmail.com

Funding information
Department of Science and Technology, Climate Change Programme (SPLICE), Government of India, Grant/Award Number: (Ref No. DST/CCP/CoE/79/2017(G))

Stationarity in the relationship between causal variables and target variables is the fundamental assumption of statistical downscaling models. However, we hypothesize that this assumption may not be valid in a changing climate. This study develops a downscaling technique in which the relationship between causal and target variables is considered to be *time-varying* rather than static. The proposed time-varying downscaling model (TVDM) is utilized to downscale monthly precipitation over India to $0.25 \times 0.25°$ gridded scale using the large-scale outputs from multiple general circulation models (GCMs), namely the Hadley Centre Coupled Model version 3 (HadCM3), coupled Hadley Centre Global Environmental Model version 2-Earth System model (HadGEM2-ES) and Canadian Earth System Model version 2 (CanESM2). Observed precipitation data are obtained from the India Meteorological Department (IMD), Pune. For future projection, the temporal evolution of each of the TVDM parameters is investigated using its deterministic (trend and periodicity) and stochastic components. TVDM is found to outperform the most commonly used statistical downscaling model (SDSM) and regional climate model (RCM) output at all the locations. The Regional Climate Model version 4 (RegCM4) precipitation data (RCM outputs) are obtained from the Coordinated Regional Climate Downscaling Experiment (CORDEX) data portal supplied by Indian Institute of Tropical Meteorology (IITM), Pune. The proposed model (TVDM) differs from the existing stationarity assumption-based approaches in updating the relationship between causal and target variables over time. It is understood that parameter uncertainty is the major issue in consideration of non-stationarity. Still, the TVDM is found to be very useful in the context of climate change due to its *time-varying* component.

KEYWORDS
climate change, downscaling, non-stationarity, precipitation, time-varying downscaling model

1 | INTRODUCTION

General circulation models (GCMs) are utilized to simulate past and future climate change (Kannan & Ghosh, 2013; Zhang & Yan, 2015). Although GCMs perform satisfactory at continental scale, their performance becomes poorer as the spatial resolution is increased (Lu & Qin, 2014; Raje & Mujumdar, 2009; Tisseuil, Vrac, Lek, & Wade, 2010). Thus, GCMs are not suitable for local-scale impact assessments and therefore it is essential to downscale the GCM outputs to finer spatial resolution (Chen, Yu, & Tang, 2010; He, Chaney, Schleiss, & Sheffield, 2016; Kannan & Ghosh, 2011; Ramdas, Rehana, & Mujumdar, 2012; Wilby et al., 2000).

Downscaling is a method to convert the large-scale, low-resolution GCM simulations (~250 to ~350 km) to high spatial resolution (e.g., 10–50 km grid size). There are different methods available for the downscaling of precipitation and these have been used at various places across the world (Bordoy & Burlando, 2014; Fowler, Blenkinsop, & Tebaldi, 2007; Hellström, Chen, Achberger, & Räisänen, 2001; Hewitson & Crane, 1996). These methods can be divided into dynamical downscaling (Hewitson & Crane, 1996; Manor & Berkovic, 2015; Schmidli et al., 2007; Xue, Janjic, Dudhia, Vasic, & De Sales, 2014) and statistical downscaling (Hessami, Gachon, Ouarda, & St-Hilaire, 2008; Langousis, Mamalakis, Deidda, & Marrocu, 2015; Wilby, Dawson, & Barrow, 2002). Dynamical downscaling utilizes a regional climate model (RCM) and is based on mathematical conceptualization of physical processes (Fowler et al., 2007; Laprise, 2008; Rotach et al., 1997). Thus, the output of a RCM is physically based and this is considered the main advantage of the dynamical downscaling approach. However, the main disadvantage that hinders the applicability of this approach is its mathematical complexity. It may require super-computers but still the final output may significantly differ from the actual observations (Giorgi, Gutowski, & William, 2015; Hellström et al., 2001; Rotach et al., 1997). The stationarity issue in RCMs has been addressed in recent studies and proposed for bias correction (Bellprat, Kotlarski, Lüthi, & Schär, 2013; Maraun, 2012). On the other hand, statistical downscaling is computationally less intensive as compared to the dynamical downscaling. Outputs from both these approaches are widely implemented in local-scale hydrological studies with more or less similar performance (Chu, Xia, Xu, & Singh, 2010; Pervez & Henebry, 2014; Teutschbein, Wetterhall, & Seibert, 2011). Maraun et al. (2015) have compared both dynamical and statistical downscaling methods through a systematic validation framework (VALUE network). However, the statistical downscaling consists of three inherent assumptions: (a) the target variable is a function of the causal variable, (b) the climate is completely represented by the causal variables and (c) the relationship between the causal variables and the target variable obtained from the historical period is stationary (Ghosh & Mujumdar, 2008; Hewitson & Crane, 1996; Wilby et al., 2002). The third assumption is practically questionable under a changing climate scenario (Ghosh & Mujumdar, 2008). It is also confirmed from the recent literature that the relationship between the causal variables and the target variable vary over time, that is, non-stationary (Duan et al., 2012; Hertig & Jacobeit, 2013; Merkenschlager, Hertig, & Jacobeit, 2017; Rashid, Beecham, & Chowdhury, 2016). Raje and Mujumdar (2010) discussed the sources of such non-stationarity in the downscaling. Hertig and Jacobeit (2013) proposed a method for statistically downscaling precipitation events considering the non-stationarity issue. Mullan, Chen, and John (2016) compared point climate change model and statistical downscaling model (SDSM) under non-stationary conditions. Merkenschlager et al. (2017) incorporates the non-stationary behaviour of the large-scale circulation with in the statistical downscaling and found that the results are improved when compared to the stationary-based models. The non-stationarities are identified between the predictor–predictand relationships (PPRs) using multiple linear regression techniques (Duan et al., 2012; Sachindra & Perera, 2016). However, these studies are not updated the PPRs at every time step. The present study uses the Bayesian paradigm in which the causal–target relationship updated at each time step, and it is an advancement as compared to the existing studies.

It is clear from the literature that the non-stationary behaviour between the causal–target variables is unavoidable in the context of climate change (Duan et al., 2012; Merkenschlager et al., 2017; Sachindra & Perera, 2016). However, the mentioned studies identified the non-stationarity considering the historical data only and the effect of non-stationarity is not assessed during the future period. The proposed approach in this study is able to overcome the stationarity assumption of statistical downscaling approaches using the skill of the Bayesian approach in updating the parameters.

The objective of this article is to develop a time-varying downscaling model (TVDM), which will be able to consider the *time-varying* relationship between the causal variables and the target variable, if one exists. Mathematical details are provided in the next section. To assess this method, downscaling is carried out over India at 0.25° lat. × 0.25° lon. resolution using outputs from multiple GCMs with different resolutions, namely (a) Hadley Centre Coupled Model version 3 (HadCM3), (b) Hadley Centre Global Environmental Model (version 2)-Earth System model (HadGEM2-ES) and (c) Canadian Earth System Model version 2 (CanESM2).

As an application, downscaling of monthly precipitation is attempted through TVDM and different aspects are explored. The performance of TVDM is also compared with the existing Statistical Downscaling Model version 5.2 (SDSM5.2) and the Regional Climate Model version 4 - (RegCM4) precipitation data (hereinafter referred to as Coordinated Regional Climate Downscaling Experiment, i.e., CORDEX) to explore the effectiveness of the developed TVDM.

2 | STUDY AREA

The entire landmass of India is considered as the study area (Figure 1). Being the seventh largest country in the world, the study area consists of a wide variation of climatological conditions; ranging from desert (Rajasthan) to the snow covered Himalayan region, very low rainfall region (Jaisalmer) to world's maximum rainfall region (Cherrapunji). Broadly, there are six wide varieties of

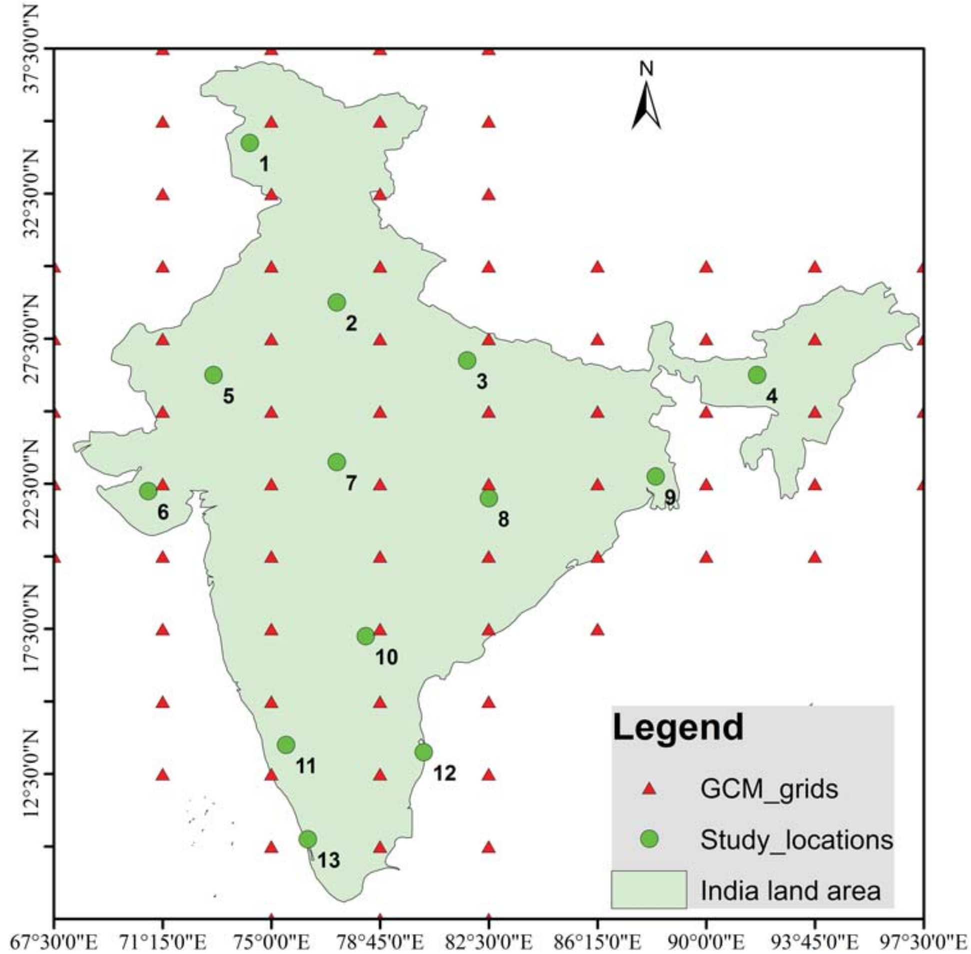

FIGURE 1 Study area map showing locations (circles) selected to compare the outputs of TVDM with rawGCM, SDSM and CORDEX along with the GCM grid points (triangles)

climatic conditions in India. The major portion (around 80%) of rainfall is contributed from the southwest monsoon (Maity & Nagesh Kumar, 2006; Singh, 2006). The annual rainfall varies from ~450 mm in Rajasthan (western state) to around 2,800 mm in Assam (eastern state) and ~1,000 mm in Jammu and Kashmir (northern state) to 3,050 mm in Kerala (southern state). There are four major seasons, that is, winter (December–February), summer (March–May), monsoon (June–September) and post-monsoon (October–November). Thus, the study area offers a wide range of climatology to test the efficacy of the proposed approaches with the existing models.

Apart from the spatial comparison over India, 10 specific key locations are also considered for location-specific discussion (Figure 1). These 10 locations are picked out in such a way that they are geographically well spread and represent the variation of Indian climate. For instance, location 1 is located in low rainfall, north Indian region and locations 2 and 3 are in sub-Himalayan region with moderate- and high-rainfall areas, respectively. Location 4 represents the dry part (west side) of the country and locations 5 and 6 represent the central Indian climate with below-normal rainfall and above-normal rainfall, respectively. Locations 7 and 9 are on the east coast, whereas locations 8 and 10 are on the west coast. The southwest monsoon strikes first on the southern part of the west coast (location 10) and due to the presence of Western Ghats, the region experiences high rainfall. Location 8 experiences rainfall during almost 8 months (May–December) because the region experiences southwest monsoon from June to September and the northeast monsoon (also known as return monsoon) from October to December.

3 | DATA USED

3.1 | Observed precipitation

Daily precipitation data were obtained at a spatial resolution of $0.25 \times 0.25°$ for India from India Meteorological Department (IMD), Pune. There are 1,803 rain gauge stations (with a minimum 90% data availability), which have been utilized for development of the gridded data (Rajeevan, Bhate, Kale, & Lal, 2006). The daily precipitation values are accumulated over months to obtain the monthly rainfall. Monthly data were obtained for the period 1951–2005. The first 40 years (1951–1990) of data have been used for model development and the remaining 15 years (1991–2005) data have been considered for model testing.

3.2 | GCM data

The outputs from three GCMs, viz. HadCM3, HadGEM2-ES and CanESM2 are used in this study. The details of each of these GCMs are as follows.

HadCM3 is a coupled atmosphere–ocean GCM and developed at the Hadley Centre in the UK Meteorological Office. The atmospheric component of HadCM3 has 19 pressure levels with a horizontal resolution of 2.5° lat. × 3.75° lon. (Gordon et al., 2000; Pope, Gillani, Rowntree, & Strattom, 2000). The HadCM3 is one of the most commonly used models in the Intergovernmental Panel on Climate Change (IPCC) Third, Fourth and Fifth Assessment Reports. HadCM3 performs adequately well and ranks higher than the other models without using flux adjustments (Reichler & Kim, 2008). The output of HadCM3 are particularly useful in studies concerning the detection and attribution of climate changes because it was able to capture the changing climate in the past owing to the natural and anthropogenic forcing (Stott, Tett, Jones, & Allen, 2000). The outputs of HadCM3 are used in many studies (Chen et al., 2010; Pichuka & Maity, 2016; Ramdas et al., 2012; Sachindra, Huang, Barton, & Perera, 2014; Schnorbus, Werner, & Bennett, 2014) for downscaling various hydro-climatic variables in future.

HadGEM2-ES (henceforth HadGEM2) is also developed at the Hadley Centre in the UK Meteorological Office and has 38 pressure levels in the atmosphere (vertical). The horizontal resolution is 1.25° lat. × 1.875° lon. The outputs of HadGEM2 are used in the IPCC Fifth Assessment Report. The details of HadGEM2 can be found from Caesar et al. (2013).

CanESM2 is developed at the Canadian Centre for Climate Modelling and Analysis (CCCMA), Canada (Arora et al., 2011). The atmospheric component of CanESM2 has 22 pressure levels with a spatial (horizontal) resolution of 2.81° lat. × 2.81° lon. The details of CanESM2 can be found from Arora et al. (2011) and Pichuka and Maity (2016).

The historical and future projected monthly data of the causal variables for all the three GCMs were downloaded from the fifth phase of Coupled Model Intercomparison Project (CMIP5). It may be noted that HadGEM2 and CanESM2 provide output for all three scenarios (RCP2.6, RCP4.5 and RCP8.5), whereas HadCM3 provides outputs only for RCP4.5 scenario. All the data are available on the IPCC Data Distribution Center (DDC) web site (http://www.ipcc-data.org/sim/gcm_monthly/AR5/Reference-Archive.html). The data sets have undergone a quality control procedure and are used in the IPCC Fifth Assessment Report (IPCC AR-5). Final selection of causal variables is based on its correlation with the target variable in the study area. The six causal variables, that is, surface specific humidity (HUS), pressure at sea level (PSL), precipitation flux (PRE), zonal wind at 500 hPa (UWN), meridional wind at 500 hPa (VWN) and geopotential height at 500 hPa (GPH) are selected. Apart from these causal variables, precipitation outputs were (hereinafter referred as rawGCM) also obtained from all the three GCMs.

3.3 | CORDEX data

The precipitation outputs from RegCM4, available in CORDEX portal, are used in this study as RCM data. The CORDEX targets to coordinate the worldwide regional climate change projections (Giorgi et al., 2015; Giorgi, Jones, & Asrar, 2009; Wilcke & Lars, 2016) and is supported by the World Climate Research Programme (WCRP). It supplies the regional data by dividing the globe into 12 predefined regions, including the Arctic and Antarctic regions. The CORDEX provides the outputs of various climatic variables at a regional scale for historical and future periods in the similar manner of the CMIP5 (Nikulin et al., 2012). It may be noted that the RegCM4 is constructed using the CanESM2 outputs as boundary condition and CanESM2 is one of the GCMs used in this study as mentioned before. Thus, RegCM4 is opted from CORDEX. It is developed by the International Centre for Theoretical Physics (ICTP) at a spatial resolution of 0.5° lat. × 0.5° lon. (Giorgi et al., 2012; Li et al., 2015). Originally, the RegCM was developed to simulate the regional climate and the outputs have been utilized in several intercomparison projects to obtain the future long-term regional climate predictions (Giorgi et al., 2012). The latest version (version 4) of this model was developed in 2010. The Indian Institute of Tropical Meteorology (IITM), Pune provides the outputs from RegCM4, which is constructed for the CORDEX framework. This data (henceforth RCM data) are downloaded for the South Asia region from the IITM website (http://cccr.tropmet.res.in/home/ftp_data.jsp). The outputs were obtained for the study area during the historical and future periods for RCP4.5 and RCP8.5 scenarios.

4 | METHODOLOGY

The proposed methodology of TVDM is developed by using the skill of the Bayesian approach in updating the parameters that were earlier adopted in Bayesian dynamic linear model (West & Harrison, 1997). The Bayesian approach is used in many hydrological studies like uncertainty quantification, water quality modelling, hydroclimatic analysis, etc. (Gabriele & Mannina, 2010; Laloy, Fasbender, & Bielders, 2010; Maity & Nagesh Kumar, 2006; Nagesh Kumar & Maity, 2008; Sarhadi, Burn, Ausin, & Wiper, 2016; Tyralis & Koutsoyiannis, 2014; Vrugt, Braak, Gupta, & Robinson, 2009; Yang, Reichert, Abbaspour, & Yang, 2007). The scope of TVDM is to capture the time-varying relationship between relevant (atmospheric) causal variables and the target variable to be downscaled. The causal variables are region-specific and are selected based on their association with the target variable, that is, precipitation in this case. The methodological flowchart is presented in Figure 2. The proposed TVDM is developed at monthly scale and it is run continuously over successive months. Stepwise methodology is presented in the following section.

4.1 | Development of TVDM

Step 1. The procedure of TVDM starts with standardizing all the causal variables to transform them to a similar range. For standardizing a variable, the mean (μ) is subtracted from it and the difference is divided by the standard deviation (σ). The equations for μ and σ are as follows:

$$\mu = \frac{\sum_{i=1}^{N} x_i}{N}, \tag{1}$$

$$\sigma = \sqrt{\frac{\sum_{i=1}^{N} (x_i - \mu)^2}{N}}, \tag{2}$$

where x is the time series data; N is the total number of data points; μ and σ are the mean and standard deviation of the time series data, respectively. Henceforth, the causal variables will refer to transformed variables only.

Step 2. The downscaling expression for the target variable (Y_t) using the information of causal variables at time step t is expressed as

$$Y_t = F_t^T \Theta_t + v_t, \tag{3}$$

where F_t^T is the transpose (indicated by superscript T) of the vector of the causal variables at the tth time step; Θ_t is the parameter vector at the tth time step; v_t is the error between the observed and the downscaled value of target variable (here precipitation) at the tth time step. The error series is assumed to be normally distributed with the zero mean and unknown variance V, that is,

$$v_t \sim N(0, V). \tag{4}$$

Vector of causal variables at tth time step is given as

$$F_t = \left(1\ x_t^1\ x_t^2\ x_t^3 \ldots x_t^z\right)^T, \tag{5}$$

where $x_t^1, x_t^2, x_t^3, \ldots, x_t^z$ are the z numbers. Causal variables at the tth time step.

The parameter vector at the tth time step is given as

$$\Theta_t = \left(\overline{Y}_t\ \theta_t^1\ \theta_t^2\ \theta_t^3 \ldots\ \theta_t^z\right)^T, \tag{6}$$

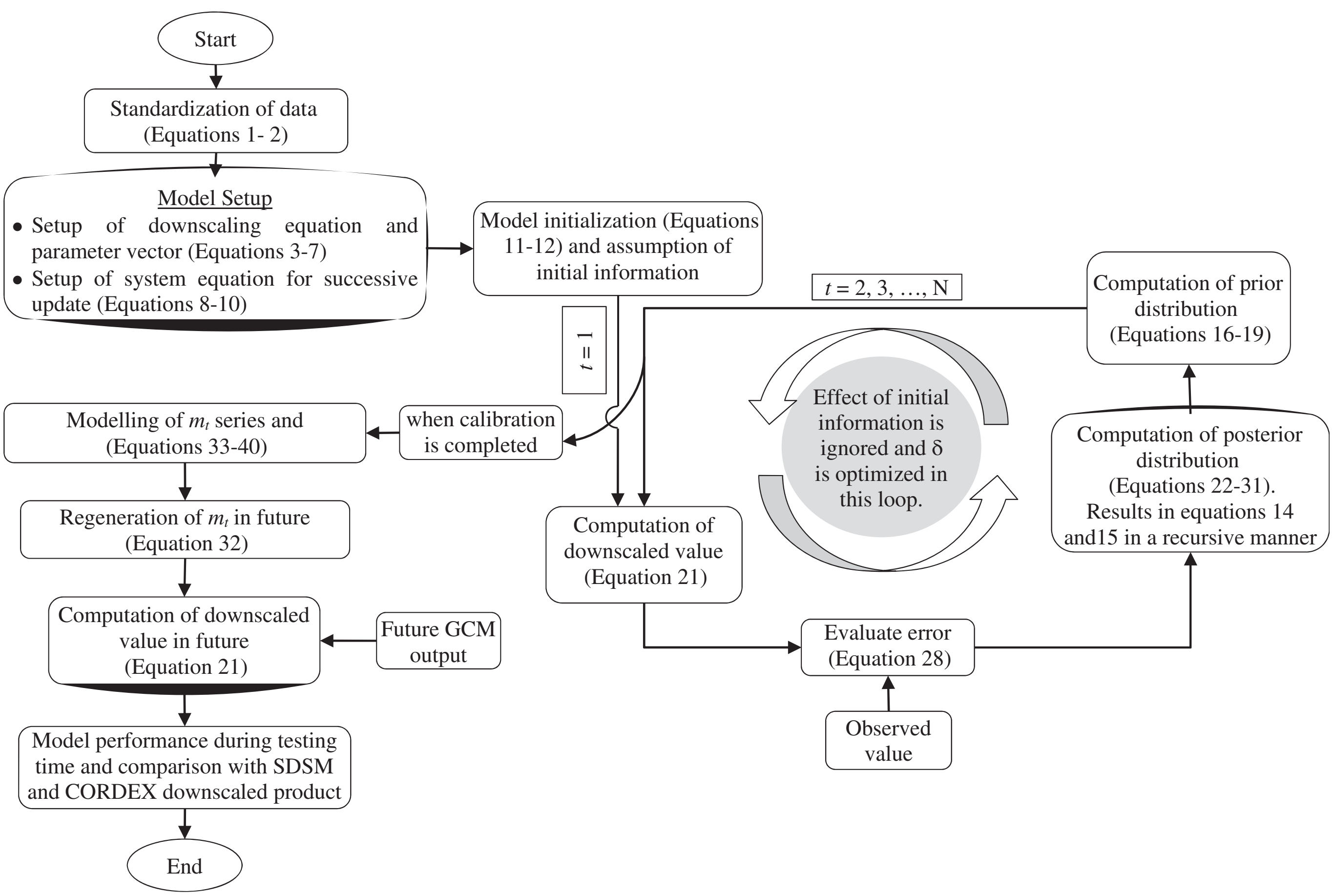

FIGURE 2 Methodological flowchart with equations as numbered in the section 4

where $\overline{Y}_t$ is the climatological mean value of the observed precipitation at tth time step. For the monthly time series, for ith month, $\overline{Y}_t$ is given as

$$\overline{Y_t} = \sum_{j=1}^{N} \left(\frac{Y_{i,j}}{N} \right), \tag{7}$$

where $Y_{i,j}$ is the value of time series at ith month (i = 1, 2, …, 12) of jth year; N is the total number of years in the development period. θ_t^1, θ_t^2, θ_t^3, $\cdots$, θ_t^z are the parameters for $x_t^1, x_t^2, x_t^3, \ldots, x_t^z$ at the tth time step, respectively.

Step 3. The successive updates of θ_t^1, θ_t^2, θ_t^3, $\cdots$, θ_t^z are carried out through the set of equations at every time step. Omitting the superscript, the general form of the system equation at the tth time step is

$$\theta_t = \theta_{t-1} + \omega_t, \tag{8}$$

where ω_t is the Student's t-distributed system evolution error with n degrees of freedom for tth time step with parameters 0 and W_t, that is,

$$\omega_t \sim T_n(0, W_t). \tag{9}$$

Degree of freedom n, for tth time step is

$$n = t - 1. \tag{10}$$

Model parameters are updated at each time step, to downscale the target time series at that particular time step.

Step 4. The modeller has to initialize the parameters at t = 1. In Bayesian paradigm, this is known as initial information, denoted as D_1. In general, that is, omitting the superscript, initial information at time t = 1 is

$$\theta_0 / D_0 \sim T_0(m_0, C_0). \tag{11}$$

Again

$$\phi / D_0 \sim G(n_0/2, d_0/2), \tag{12}$$

where ϕ is the precision parameter and defined as

$$\phi = V^{-1}. \tag{13}$$

T_0 and G stand for Student's t distribution (degree of freedom shown as subscript) and Gamma distribution, respectively. It may be noted that the precision parameter indicates how accurate the model performance is at each time step. The inverse of this parameter is used for associated uncertainty with the downscaled value. The parameters m_0, C_0, n_0 and d_0 are supplied to the TVDM as the initial information for all the causal variables. Although the selection of these initial values is subjective, their effect dissipates after some time steps. Hence, it is recommended to ignore some initial time steps from performance assessment to avoid the effect of subjective choice of initial parameters. This period can also be used as spin-up period to stabilize the initial information.

Step 5. In order to update the parameters from the time step (t − 1) to t, where t = 2, 3, 4, …, N, let us assume that posterior distribution for θ_{t-1} is

$$\theta_{t-1} / D_{t-1} \sim T_{t-1}(m_{t-1}, C_{t-1}), \tag{14}$$

$$\phi / D_{t-1} \sim G(n_{t-1}/2, d_{t-1}/2). \tag{15}$$

The posterior distribution can be viewed as the information (probabilistic) available at the end of each time step (say t), when the error made in that time step is known. This posterior distribution is used to compute the prior distribution for the next time step (i.e., t + 1), which is used by the model for downscaling at the time step t + 1. At the end of the time step t + 1, with the available information of error made, the posterior distribution for the time step t + 1 is computed and the procedure is repeated recursively. These steps are explained as follows. The prior distribution for θ_t is expressed as

$$\theta_t / D_{t-1} \sim T_t(m_{t-1}, R_t). \tag{16}$$

R_t is expressed as

$$R_t = C_{t-1} + W_t, \tag{17}$$

where W_t is known as system evolution variance at time step t. The system evolution variance is a measure of decay in information from one time step to another (i.e., t to t + 1) in the process of downscaling. This is analogous to the uncertainty for any future information and it is required to know the sequence of evolution variance W_t a priori, which may not be possible. To overcome this, R_t is expressed as

$$R_t = C_{t-1} / \delta, \tag{18}$$

where δ is known as the discount factor and vary between 0 and 1. Thus, the discount factor ensures that the system evolution variance increases from one time step to the next time step (i.e., t to t + 1), that is, uncertainty is higher in future information. Equations (17) and (18) imply that

$$W_t = C_{t-1} \left(\frac{1}{\delta} - 1 \right). \tag{19}$$

The optimum value of δ is estimated on the basis of model performance. It is also noteworthy that the higher values of δ indicate slower rate of decay of previous information and vice versa (West & Harrison, 1997).

Step 6. Finally, the downscaled target variable at time step t is expressed in the form of

$$(Y_t / D_{t-1}) \sim T_n(F_t, Q_t), \tag{20}$$

where n is as defined before for the time step t and

$$F_t = \overline{Y_t} + x_t^1 \times m_{t-1}^1 + x_t^2 \times m_{t-1}^2 + x_t^3 \times m_{t-1}^3 + \ldots + x_t^z \times m_{t-1}^z, \tag{21}$$

$$Q_t = \left(x_t^1\right)^2 \times R_t^1 + \left(x_t^2\right)^2 \times R_t^2 + \left(x_t^3\right)^2 \times R_t^3 + \ldots + \left(x_t^z\right)^2 \times R_t^z + S_{t-1}, \tag{22}$$

where R_t is defined as before, and

$$S_{t-1}=\frac{d_{t-1}}{n_{t-1}}. \tag{23}$$

Step 7. Posterior distribution for θ_t is

$$(\theta_t/D_t)\sim T_n(m_t,C_t), \tag{24}$$

where

$$m_t=m_{t-1}+A_t e_t, \tag{25}$$

$$C_t=R_t S_t/Q_t, \tag{26}$$

where A_t is given as

$$A_t=x_t R_t/Q_t, \tag{27}$$

$$e_t=Y_t-F_t. \tag{28}$$

For the next step, that is, $t+1$, n_t and d_t are required to calculate Q_t using S_t. These are expressed as

$$n_t=n_{t-1}+1, \tag{29}$$

$$d_t=d_{t-1}+S_{t-1}e_t^2/Q_t. \tag{30}$$

Thus, the distributional form of the precision parameter ϕ at time step t is obtained as

$$(\phi/D_t)\sim G(n_t/2,d_t/2). \tag{31}$$

The model parameters, $m_t^p\,(t=1,2,\cdots,n \text{ and } p=1,\cdots,z)$ (hereinafter referred as m-values) evolve over time for all the input variables.

4.2 | Application of TVDM for downscaling the future precipitation

So far, TVDM is developed based on the historical period where observed precipitation at each time step is available and calculation of error is possible at each time step that helps to estimate the prior distribution (Equation (16)) for the next time step. For future projection, it should be noted that the weather sequence resulting from free running climate models does not match with the actual observed sequence of weather. Hence, the errors will not be available for the future period. One possible solution could be the investigation of temporal evolution of the model parameters and its regeneration. Statistically, the stochastic evolution of model parameters (m-values) may be investigated during the historical period and the model parameters can be regenerated by considering its characteristics of the temporal evolution. To model the characteristics of the temporal evolution of the model parameters, both the deterministic and the stochastic components are modelled to regenerate the m-values to be used for downscaling in the future.

The linear trend and the periodicity components are the deterministic part of historical m-values time series. The stochastic part is modelled through auto-regressive (AR) model. First, the linear trend, if any, is taken out from the time series of historical m-values. Then the periodic component, wherever it is found to be significant, is extracted from the detrended time series. Therefore, an AR model is developed to model the residual series. Thus, the time series of historical m-values is modelled as

$$m_t=m_t^{tr}+m_t^{pr}+m_t^{st}, \tag{32}$$

where m_t^{tr}, m_t^{pr} and m_t^{st} represent the linear trend, periodic and the stochastic components, respectively, of the m-values at time t. The m_t^{tr} is given by

$$m_t^{tr}=p_1 t+p_2, \tag{33}$$

where p_1 and p_2 are the regression coefficients that are obtained by least square method taking time as the independent variable. After removing the trend component from the time series, the periodic component, that is, m_t^{pr} is modelled by

$$m_t^{pr}(T)=A_0+\sum_{k=1}^{h}\left[A_k\sin\left(\frac{2\pi kT}{P}\right)+B_k\cos\left(\frac{2\pi kT}{P}\right)\right], \tag{34}$$

where $m_t^{pr}(T)$ are harmonically fitted means at period T (T = 1, 2,…, P) and P is the base period, which is calculated from the periodogram of the detrended time series of m-values which is given as

$$P=\frac{2\times\pi}{w}, \tag{35}$$

where w is the index value corresponding to the peak of the periodogram; A_0 is the mean of historical m-values and is given as

$$A_0=\frac{1}{P}\sum_{T=1}^{P}[X(T)], \tag{36}$$

where $X(T)$ is the time series of detrended m-values; h is the total number of harmonics, which is expressed as

$$h=\begin{cases} P/2 & \text{for even values of } P \\ (P-1)/2 & \text{for odd values of } P \end{cases}. \tag{37}$$

A_k and B_k are sine and cosine Fourier coefficients, respectively, and given as

$$A_k=\frac{2}{P}\sum_{T=1}^{P}\left[X(T)\times\sin\left(\frac{2\pi kT}{P}\right)\right], \tag{38}$$

$$B_k=\frac{2}{P}\sum_{T=1}^{P}\left[X(T)\times\cos\left(\frac{2\pi kT}{P}\right)\right], \tag{39}$$

where k = 1, 2, …, h.

After removing the trend and periodicity from the time series, the residual is modelled by an AR model. The order of the AR model is decided by the auto-correlogram and partial auto-correlogram. In general, AR(1) model may found to be sufficient after removing the trend and the periodicity. Thus, the stochastic component is modelled as

$$m_t^{st} = b \times m_{t-1}^{st} + m_t^e, \tag{40}$$

where m_t^{st} is the modelled stochastic component, b is the coefficient of the AR(1) model fitted to the residuals and m_t^e is the error at the tth time step. The error m_t^e is assumed to be normally distributed with a zero mean and a standard deviation of σ_{e_t}. Using the values from Equations (33), (34) and (40) in Equation (32), ensembles of many realizations can be generated. One realization can be used at a time to get a realization of the downscaled precipitation. Thus, an ensemble of realizations of downscaled precipitation can be obtained. The process may generate a few negative values as well that can be truncated to zeros.

4.3 | Comparison between the performance of TVDM, SDSM and RCM

The performance of the TVDM is compared with the performance of existing SDSM5.2 and the CORDEX data. For fair comparison of results, all the model outputs (RCM, TVDM and SDSM) are bias-corrected before comparison. The bias correction factors are calculated using the ratio of long-term monthly mean of observed data and downscaled (RCM, TVDM and SDSM) data from the development period as per Maraun (2012). These bias correction factors are further utilized in the testing and future periods to obtain the bias-corrected downscaled (RCM, TVDM and SDSM) values during respective periods. The SDSM calculates statistical relationships, based on the multiple linear regression techniques, between the large-scale (causal variables) and the local-scale (target) climate data (Wilby et al., 2002). These relationships between the causal variables and the target variable are developed based on historical data and assumed to remain the same in the future also. These relationships can be used to obtain downscaled local information for future time periods by driving the relationships with GCM-derived causal variables. Further details on SDSM can be found in the literature (Wilby et al., 2002; Wilby & Dawson, 2013).

The causal variables and the rawGCM precipitation data are obtained at each target location (finer grid intersection at $0.25 \times 0.25°$) through inverse distance weighting method (IDWM) from four surrounding GCM grids of that target location. IDWM is a deterministic approach to compute the value of a variable at a point where it is not known using the information from nearby points where its values are known (Shepard, 1968). Inverse of the square of the distance is used as the weightage factor in IDWM. Then the association between the observed, GCM (hereinafter referred as rawGCM to emphasize "no downscaling"), CORDEX data and downscaled precipitation using SDSM and TVDM (all bias-corrected as mentioned before) is assessed through different statistical measures like mean (μ), root-mean-square error (RMSE), un-biased RMSE (ubRMSE), Nash-Sutcliffe efficiency (NSE), degree of agreement (D_r), standard deviation (σ) and 95th percentile value. The lesser the difference (error) between the observed and downscaled μ, σ and 95th percentile values, the better is the performance of the model. Similarly, the lower values of RMSE and ubRMSE indicate better performance of the model. Higher values of NSE and D_r (closer to +1) signifies superior performance of the model when compared to the observed data.

5 | RESULTS AND DISCUSSION

5.1 | Performance of the models during development period

In this section, first, the association among observed and rawGCM precipitation is checked. Then the calibration of proposed TVDM is explained and subsequently its performance is assessed. Next, the performance of existing models such as SDSM and CORDEX are examined. Finally, the performance of TVDM is compared with the rawGCM, SDSM and CORDEX outputs.

5.1.1 | RawGCM precipitation versus observed precipitation (calibration period)

First, the association between the rawGCM precipitation and the observed precipitation is checked at each location. As expected, the correspondence between rawGCM precipitation and the observed precipitation is very poor (Figures 3–5). The values of NSE and D_r are varying from −0.15 (location 9) to 0.62 (location 6) and 0.58 (location 9) to 0.77 (location 6), respectively, in case of HadCM3 (Figure 3). The wide variation of RMSE (ubRMSE) is also noticed and found to vary between 90.05 mm (84.44 mm) to 277.30 mm (218.96 mm). The mean values are varying between 28.37 mm to 140.70 mm (Figure 3). The association between rawGCM and observed precipitation is also found poor using HadGEM2 (Figure 4) and CanESM2 (Figure 5) outputs. For instance, the minimum NSE value is noted as −0.27 at location 9 for HadGEM2 (Figure 4) and −0.26 at location 10 for CanESM2 (Figure 5). As an example, the scatterplot between the observed and the rawGCM (HadCM3) at location 6 is presented in Figure S1a, Supporting information in case of HadCM3. It seems that the GCM underestimates the higher precipitation values occurring in the monsoon months (June–September). This is true for all the locations. Thus, the correspondence between rawGCM values and the actual observed precipitation is poor (Figures 3 and S1).

5.1.2 | Calibration of TVDM

The proposed TVDM has been calibrated by considering 40 years of monthly precipitation data from 1951 to 1990 (development period). All the six causal variables along with the observed precipitation are utilized to calibrate the

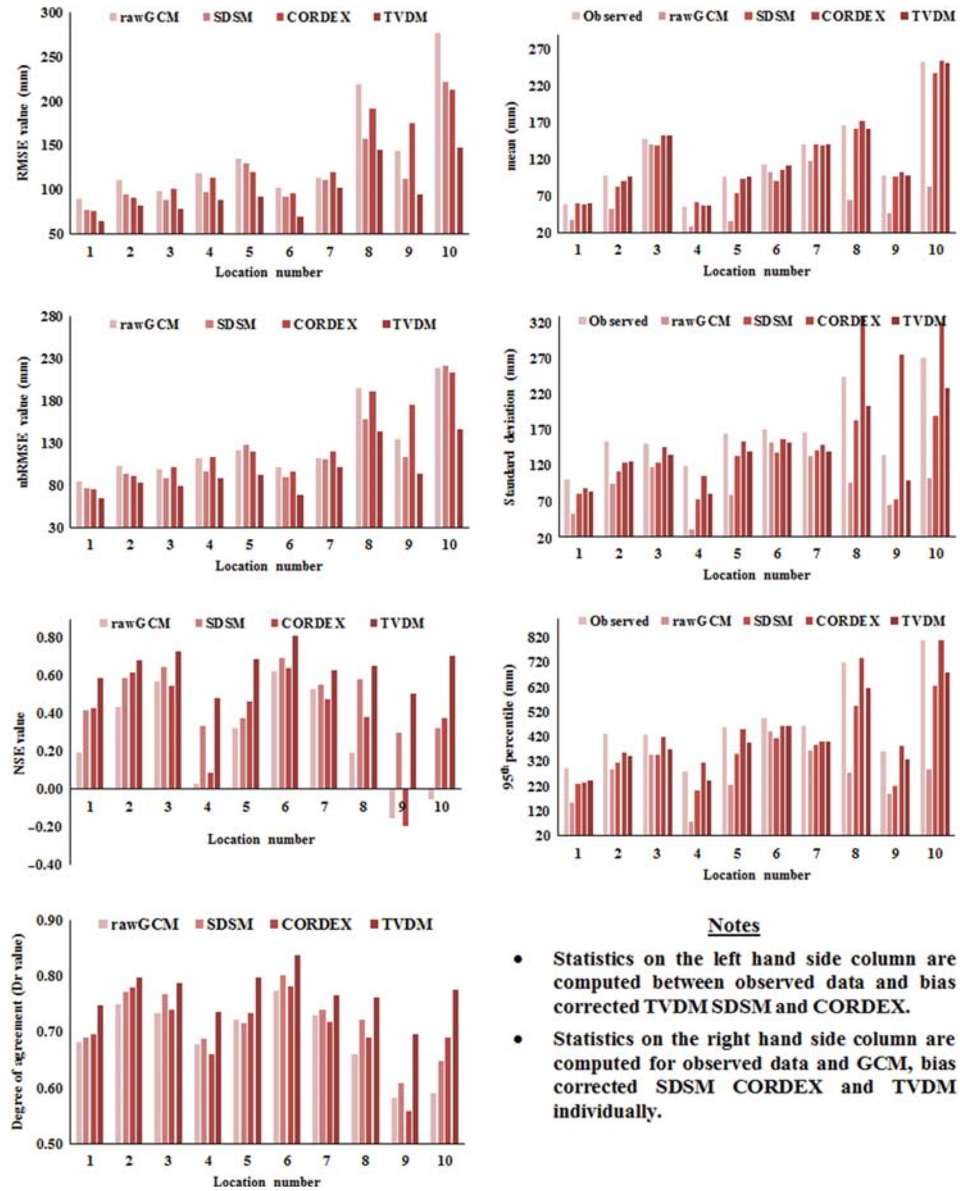

FIGURE 3 Statistical measures obtained from various models during development period (1953–1990) using HadCM3 outputs [Colour figure can be viewed at wileyonlinelibrary.com]

TVDM. Subjective assumptions of initial parameters are required for initializing the TVDM. In this study, five different sets of initial parameters are considered. The output series are compared against each other for the first 7 years, that is, initial 84 months (for visual convenience only). As a sample plot, the comparative plots along with different sets of initial values are shown in Figure S2. Although the initial assumption of model parameters affects the output, it is noticed that output series of different sets are converging with each other approximately after 18 time steps, that is, one and a half years (Figure S2). Thus, in general, initial 2-year period is excluded while evaluating the model performance to avoid the effect of the initial assumption of parameters. Therefore, the development period is considered as 1953–1990. The discount factor (δ) plays a vital role while developing the TVDM. The optimum value of the discount factor $\delta$is obtained as 0.92. The discount factor (δ) is kept the same in all the five sets of initial parameters mentioned before.

5.1.3 | Performance of the proposed TVDM (calibration period)

The precipitation is downscaled and bias-corrected for India using TVDM at a spatial resolution of $0.25 \times 0.25°$. First, the performance of the TVDM is evaluated in terms of the statistical measures mentioned before at all the 10 selected locations across India using outputs from HadCM3 as input (Figure 3). The RMSE (ubRMSE) values range between 64.15 mm (64.02 mm) to 147.11 mm (146.79 mm). The values of D_r varies from 0.70 (location 9) to 0.84 (location 6). The other statistical measures like NSE, μ, $\sigma$and 95th percentile values are found to be improved as compared to the rawGCM precipitation (see Figure 3). As a sample plot, the scatterplot during the development period has been presented in Figure S1d between observed and TVDM downscaled precipitation for location 6.

The consistency of the TVDM in downscaling precipitation is checked by using other GCM outputs as well. The results obtained from HadGEM2 and CanESM2 are

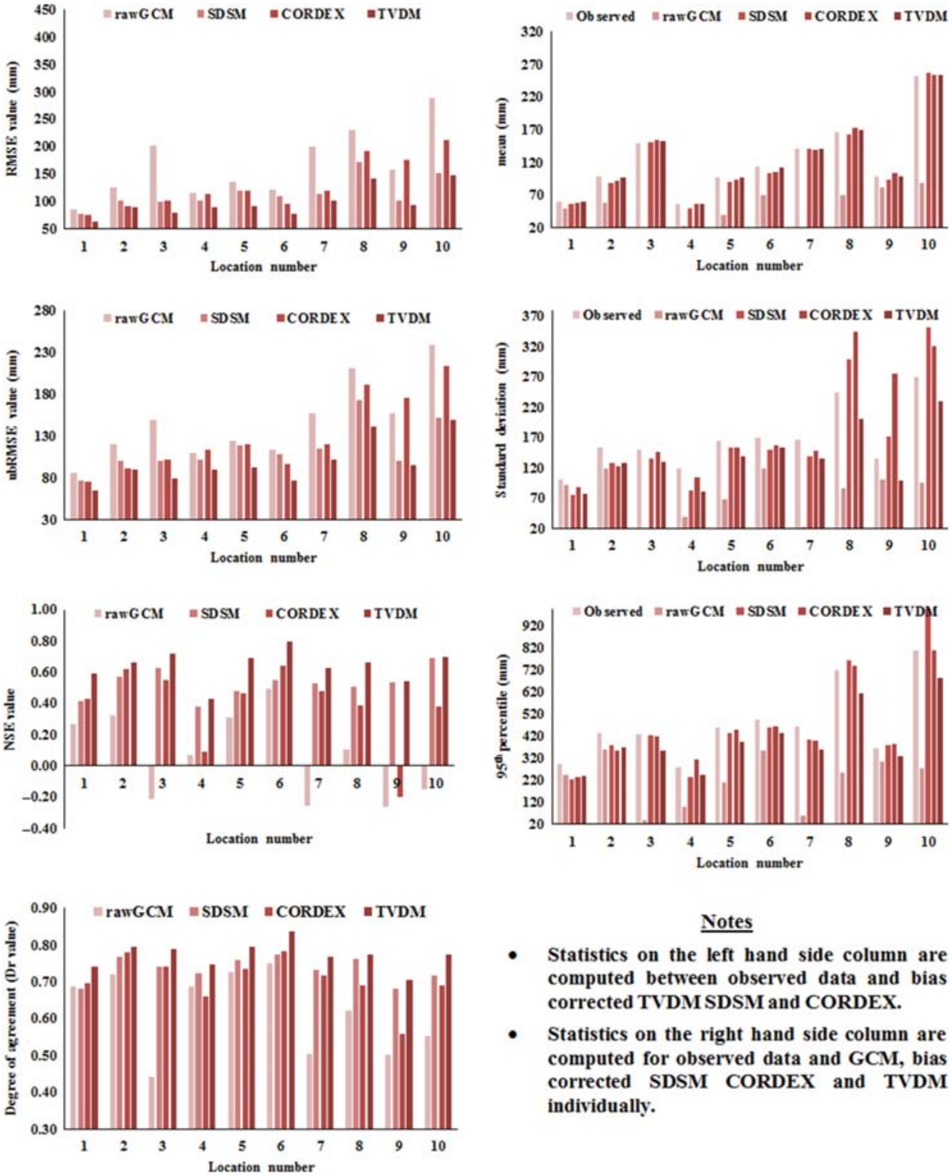

FIGURE 4 Statistical measures obtained from various models during development period (1953–1990) using HadGEM2 outputs [Colour figure can be viewed at wileyonlinelibrary.com]

shown in Figures 4 and 5. The results reveal that the performance of TVDM is consistent across different locations with widely varying climatology for all the GCMs used. For instance, mean values (in "mm") at low-rainfall (location 4), normal-rainfall (location 2) and high-rainfall (location 10) regions during calibration period using HadGEM2 (CanESM2) outputs are noted as 53.36 (56.76), 97.13 (95.13) and 253.86 (255.43), respectively (refer to Figures 4 and 5). The NSE in the mentioned locations are noted as 0.43 (0.44), 0.66 (0.67) and 0.70 (0.71), respectively. The values of D_r at respective locations are noted as 0.75 (0.75), 0.79 (0.80) and 0.77 (0.78) using HadGEM2 (CanESM2), respectively (refer to Figures 4 and 5).

5.1.4 | Performance of the existing SDSM and CORDEX (calibration period)

While using SDSM for downscaling, it is worth mentioning that the input data for SDSM at every individual location has to be provided separately (manually). Thus, it is very difficult to downscale the precipitation at all the grid intersections in India (contains thousands of grid intersections) using SDSM. Therefore, downscaling is carried out using SDSM only at those 10 key locations (shown in Figure 1). Next, as mentioned in section 3, the precipitation outputs from CORDEX are procured from IITM for the study region. Downscaled precipitations are bias-corrected before assessing the performance.

The statistical measures of association between the observed and the downscaled precipitation using SDSM and CORDEX during development period are represented in Figure 3 (HadCM3). The best values of RMSE and ubRMSE are observed in the low-rainfall regions (locations 1, 4 and 9). The SDSM outputs found to perform better in comparison to the rawGCM at almost all the locations. Performance of SDSM and CORDEX are more or less same considering all the locations across India. The mean value of SDSM is found to match better with the normal- and high-rainfall locations. The CORDEX seems to be overestimating in high-rainfall locations (except location 6) and it is

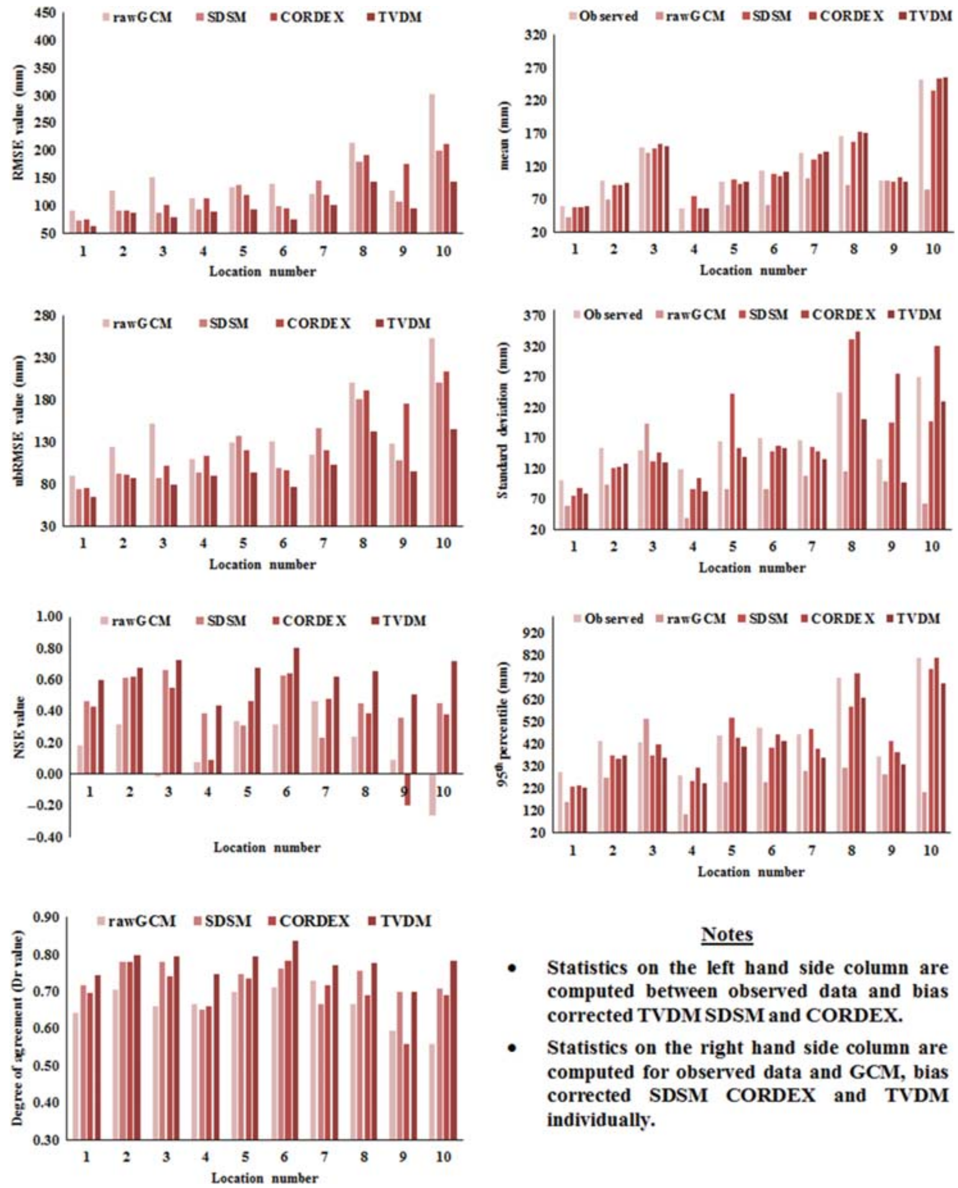

FIGURE 5 Statistical measures obtained from various models during development period (1953–1990) using CanESM2 outputs [Colour figure can be viewed at wileyonlinelibrary.com]

underestimating in normal- and low-rainfall regions (Figure 3). Furthermore, the performance of the CORDEX is noted as very poor in the southern part of India (locations 8, 9 and 10) and its performance at moderate-rainfall regions (locations 1, 2 and 5) is better when compared to rawGCM and SDSM (as per NSE, D_r and 95th percentile values). The mean values are also matching better with the observed precipitation mean. For instance, the mean values at normal-rainfall (location 2) and high-rainfall (location 8) regions are noted as 97.99 and 165.85 mm in case of observed data, whereas these are noted as 82.35 and 161.74 mm from SDSM output and 91.16 and 172.58 mm from CORDEX output, respectively, at corresponding locations. The high values of the standard deviations are noticed using the SDSM outputs over high-rainfall regions (particularly south Indian locations). It implies high uncertainty in the SDSM and CORDEX at these locations. Overall, a comparison between the rawGCM data and the downscaled precipitation using SDSM and CORDEX indicates that the SDSM and CORDEX outputs correspond better to the observed precipitation. The consistency is noticed from the outputs of other GCMs, that is, HadGEM2 and CanESM2 whose association with the observed precipitation and CORDEX precipitation are presented in Figures 4 and 5, respectively.

5.1.5 | Comparison of TVDM outputs with rawGCM, SDSM and CORDEX (calibration period)

The TVDM downscaled precipitation corresponds better to the observed data and found to be much improved while comparing with both SDSM and CORDEX. For instance, the values of μ, σ and 95th percentile using TVDM are found to be very close to the observed data (refer to Figures 3–5). The best values of NSE and D_r are noted as 0.81/0.79/0.80 and 0.84/0.84/0.84 using HadCM3/HadGEM2/CanESM2 GCMs, respectively, at location 6. The same values corresponding to location 6 are noted as 0.62/0.49/0.32 and 0.77/0.75/0.71 using rawGCM and 0.69/0.55/0.63 and 0.80/0.77/0.76 using SDSM downscaled precipitation, respectively, for respective GCMs. These

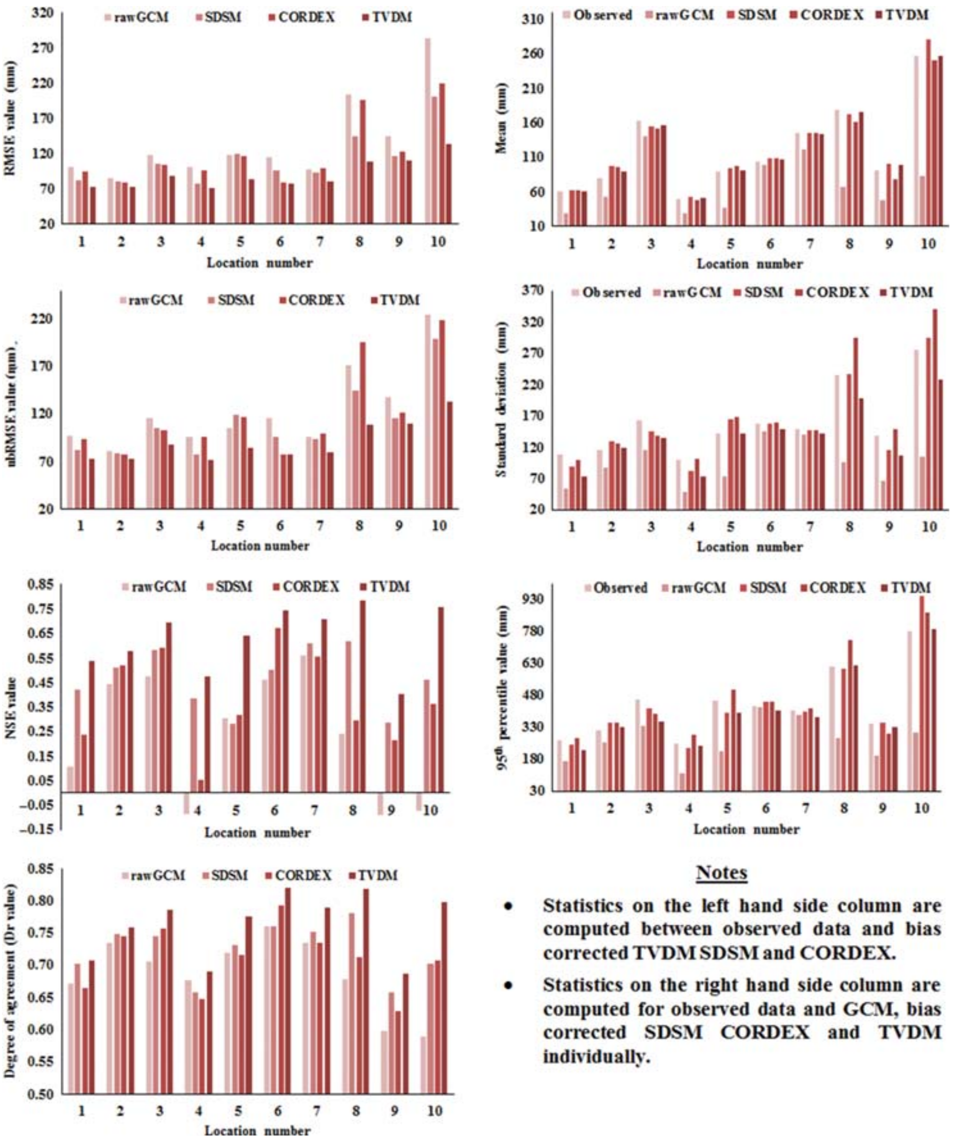

FIGURE 6 Visual variation of statistical measures obtained from various models during testing period (1991–2005) using HadCM3 outputs [Colour figure can be viewed at wileyonlinelibrary.com]

values are found to be 0.64 (NSE) and 0.78 (D_r) using CORDEX output, respectively. As an example, the association of these outputs with observed precipitation at location 6 are shown as scatterplots in Figure S1. It is noticed from Figure S1 that the CORDEX (panel b) and SDSM (panel c) outputs slightly overestimate during the dry months (November–May) and considerably underestimate during the monsoon months (June–October). On the other hand, the TVDM downscaled precipitation matches to the observed data with much better accuracy as compared to the output from other models (panels a–c). The performance of the TVDM is consistently good at all the locations (Figures 3–5) and its performance is outstanding at medium and high-rainfall regions (locations 2, 3, 5, 6, 8 and 10). Overall, it can be inferred that the downscaled precipitation using TVDM corresponds well to the observed precipitation and it is superior to the rawGCM as well as outputs from SDSM and CORDEX.

5.2 | Performance during testing period

5.2.1 | Downscaling in future using TVDM: Modelling of parameter series

While modelling the parameter series during the calibration period to extract the stochastic properties, the latest 35 years (1956–1990) period is used. Latest 35 years are used to ensure to extract the recent climatological trend. More than 30 years will reveal more confident estimate in case of a stationary series. However, it is noticed that some climate variables are found to change more rapidly over last couple of decades. Again, according to the World Meteorological Organization (WMO), it is also not recommended to consider shorter than 30-year period to assess the climatological properties. Thus, latest 35 year period is used for extracting the stochastic properties. Consideration of the stochastic properties from the latest period will ensure the maximum time horizon in future for projection.

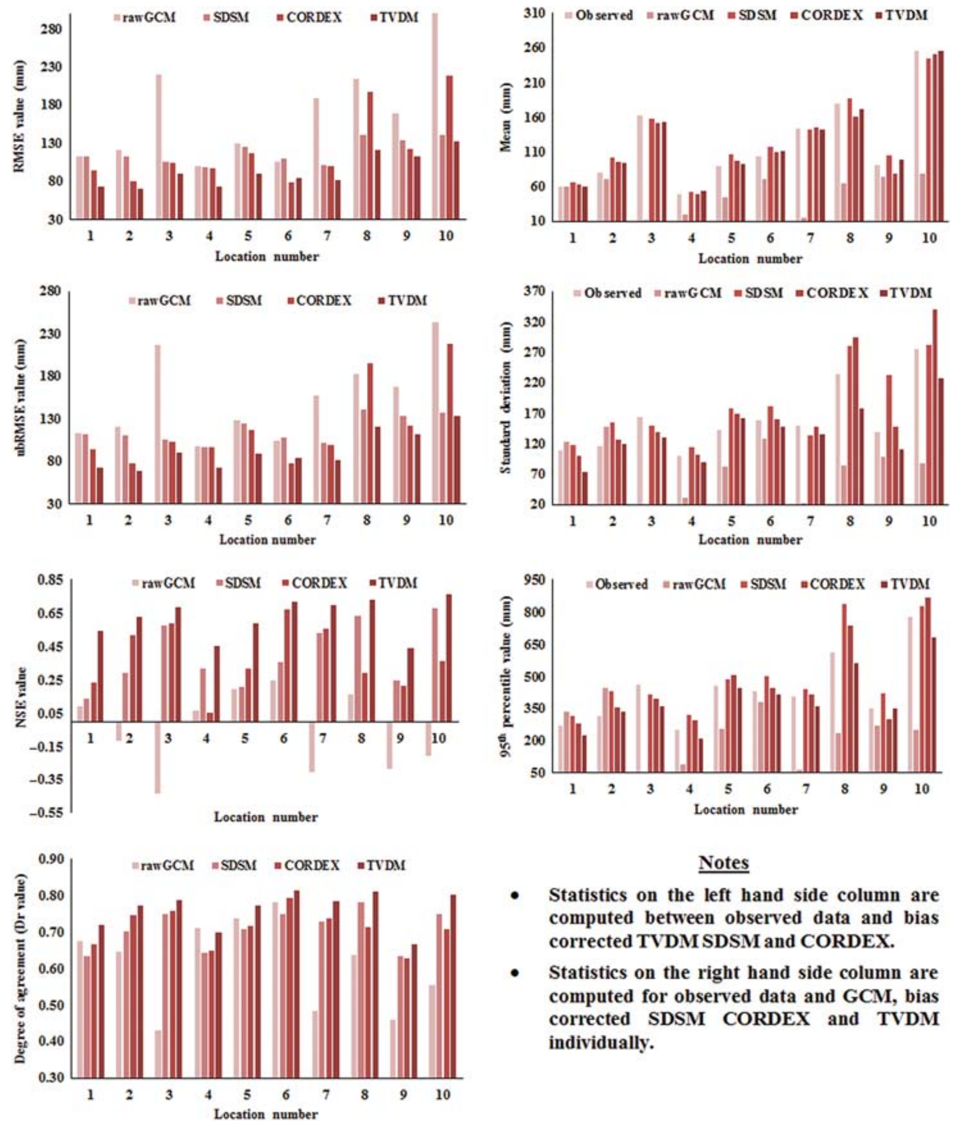

FIGURE 7 Statistical measures obtained from various models during testing period (1991–2005) using HadGEM2 outputs [Colour figure can be viewed at wileyonlinelibrary.com]

For brevity, one parameter (U-wind, that is, m_UWN) at location 6 is used for demonstration and corresponding plots are presented in Figure S3. First, the trend (panel a) and periodicity (panel b), if any, is removed. Next, the residual (panel c) is modelled with an AR(1) model. Adding these three components (Equation (32)), 20 realizations are regenerated. One such typical realization of *m*-values for each of the six causal variables is shown in Figure S4 for location 6. In Figure S4, the blue line indicates the series of *m*-values during the model development period (1956–1990) and testing period (1991–2005) knowing the observed precipitation. Red line indicates the expected value (out of 20 ensembles) of regenerated *m*-values (without knowing the observed precipitation) during testing period (1991–2005) by considering the trend, periodicity and the stochastic component of the *m*-value series during the development period. It is noticed that the regenerated *m*-values (1991–2005) preserves the stochastic properties and corresponds well with the expected *m*-values during the testing period. The procedure is repeated at each grid intersection to regenerate the *m*-values and used for downscaling in future at that corresponding grid intersections.

5.2.2 | Performance of the TVDM with rawGCM, SDSM and CORDEX (testing period)

The skill of proposed TVDM is tested before applying it to obtain the future downscaled precipitation. Therefore, the downscaled precipitation using the regenerated *m*-values and causal variables is compared during the testing period (1991–2005) when the observed precipitation data are available which helps to test the model efficacy. The location-wise statistical measures between observed precipitation and the downscaled precipitation (using HadCM3) obtained from rawGCM, SDSM, CORDEX and TVDM are calculated during the testing period (Figure 6). The best values of D_r and NSE are noticed in case of TVDM model at all the selected key locations (refer Figure 1). For instance, the maximum and minimum D_r values using TVDM are found

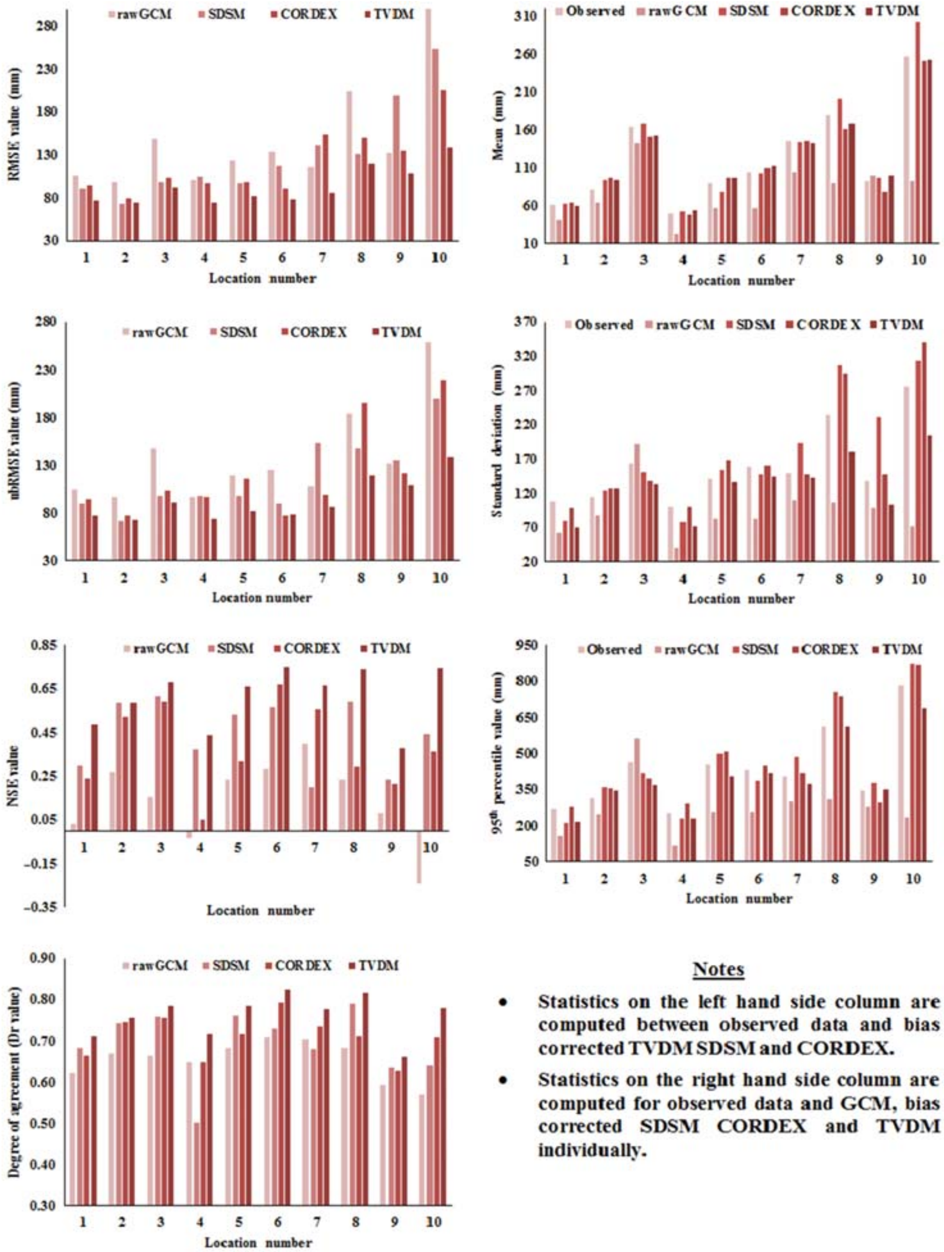

FIGURE 8 Statistical measures obtained from various models during testing period (1991–2005) using CanESM2 outputs [Colour figure can be viewed at wileyonlinelibrary.com]

as 0.83 (location 6) and 0.69 (location 9) and at these locations the corresponding values of D_r are noted as 0.80 and 0.66 (using SDSM), 0.79 and 0.63 (using CORDEX) and 0.76 and 0.60 (using rawGCM). The mean and standard deviation values calculated during the testing period are compared with the observed mean and standard deviation values at the key locations and TVDM found to be best performing. For instance, the mean values (in mm) at location 10 (high-rainfall region) are noted as 256.10 (observed data), 82.59 (rawGCM), 280.10 (SDSM), 250.95 (CORDEX) and 255.94 (TVDM), respectively. Similarly, the mean values at low-rainfall region (location 4) are obtained (in mm) as 48.64 (observed data), 29.45 (rawGCM), 53.34 (SDSM), 48.28 (CORDEX) and 51.35 (TVDM), respectively. The SDSM outputs revealed that it is overestimating in the low-rainfall locations (see locations 1, 4 and 9 in Figure 6) and satisfactory performance is perceived in normal- and high-rainfall locations. In brief, the performance of proposed TVDM is found to be superior to the rawGCM, SDSM and CORDEX outputs at all the locations (Figure 6). The other statistical measures (RMSE, ubRMSE, NSE and 95th percentile) are also presented in Figure 6 reveals the same fact. As a sample plot, the association between observed precipitation and modelled precipitation using rawGCM, SDSM, CORDEX and TVDM outputs is presented as scatterplot in Figure S5. The better correspondence between observed and downscaled precipitation in case of TVDM is noticed from these scatterplot (panel d).

Similarly, the performance using HadGEM2 and CanESM2 during testing period is presented in Figures 7 and 8, respectively. From these plots, the superior performance of TVDM as compared to SDSM and CORDEX is found at all the key locations. For instance, the NSE value at location 6 is noted as 0.35 (SDSM), 0.67 (CORDEX) and 0.72 (TVDM) using HadGEM2 (Figure 7) outputs and

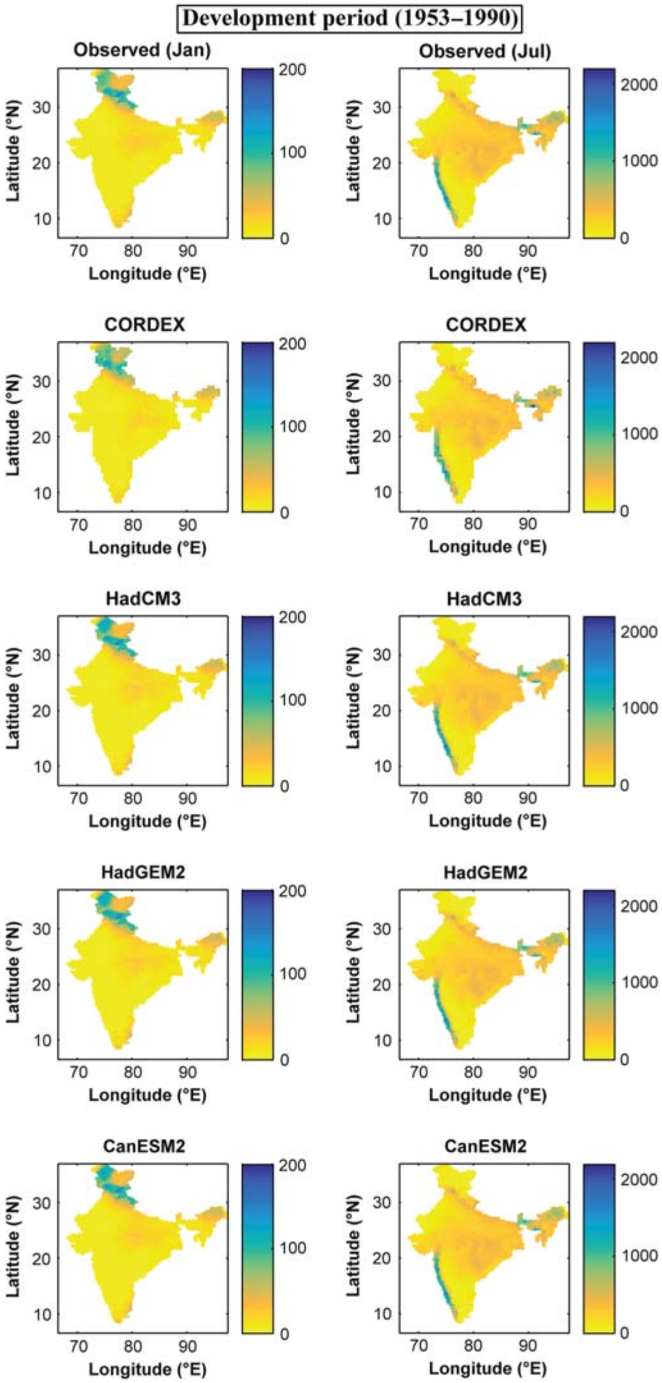

FIGURE 9 Comparison between observed precipitation and bias-corrected TVDM (using HadCM3, HadGEM2 and CanESM2) and CORDEX precipitation during development period through monthly average precipitation in the January (left panel) and July (right panel) months [Colour figure can be viewed at wileyonlinelibrary.com]

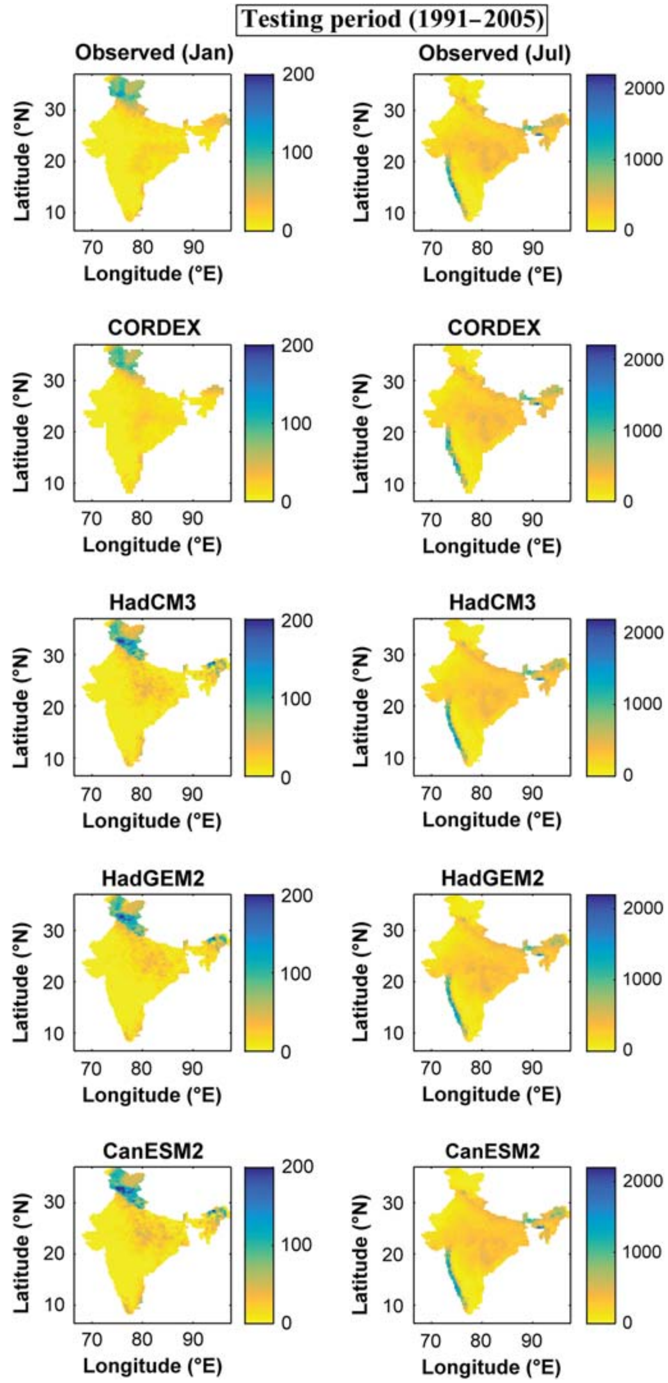

FIGURE 10 Comparison between observed precipitation and bias-corrected TVDM (using HadCM3, HadGEM2 and CanESM2) and CORDEX precipitation during testing period through monthly average precipitation in the January (left panel) and July (right panel) months [Colour figure can be viewed at wileyonlinelibrary.com]

the same is noted as 0.56 (SDSM), 0.67 (CORDEX) and 0.75 (TVDM), respectively, using CanESM2 (Figure 8) outputs. The other performance measures like mean, RMSE, ubRMSE, D_r, standard deviation and 95th percentile values are also revealed the superiority of TVDM across all over selected key locations of India (Figures 7 and 8).

5.3 | Application of TVDM in downscaling the precipitation for entire India and comparison with CORDEX data

The analysis is extended to the entire Indian landmass for downscaling the precipitation. The TVDM downscaled precipitation is contrasted with the CORDEX data during the model

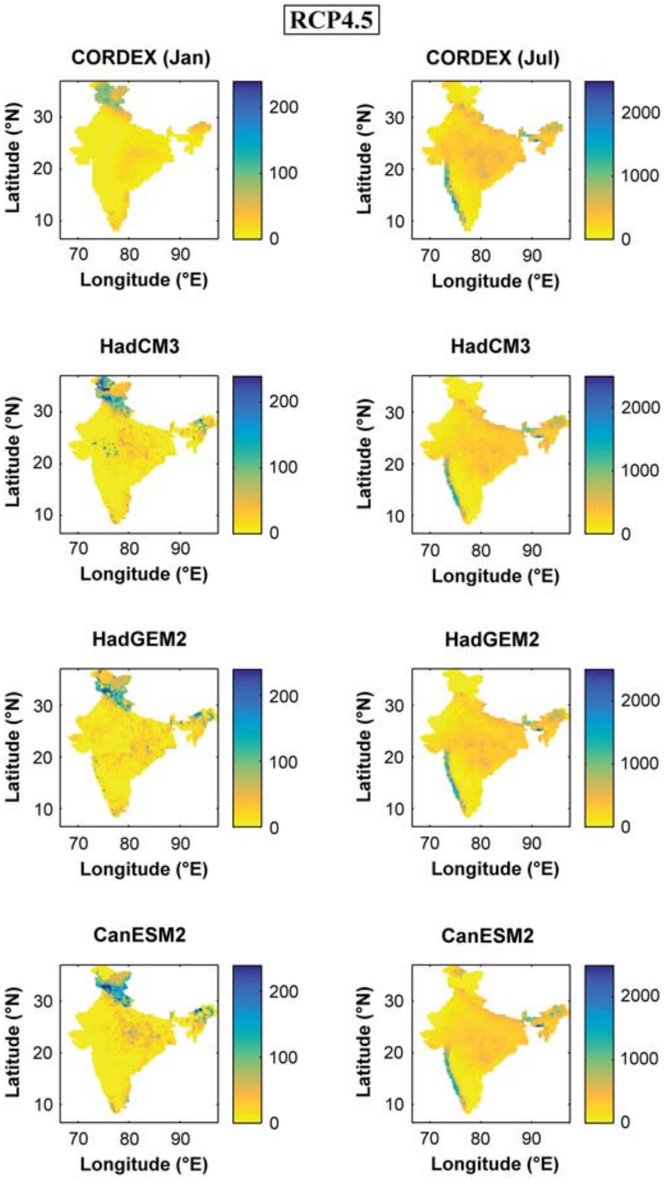

FIGURE 11 Comparison between bias-corrected TVDM (using HadCM3, HadGEM2 and CanESM2) and CORDEX precipitation during future period using RCP4.5 scenario outputs through monthly average precipitation in the January (left panel) and July (right panel) months [Colour figure can be viewed at wileyonlinelibrary.com]

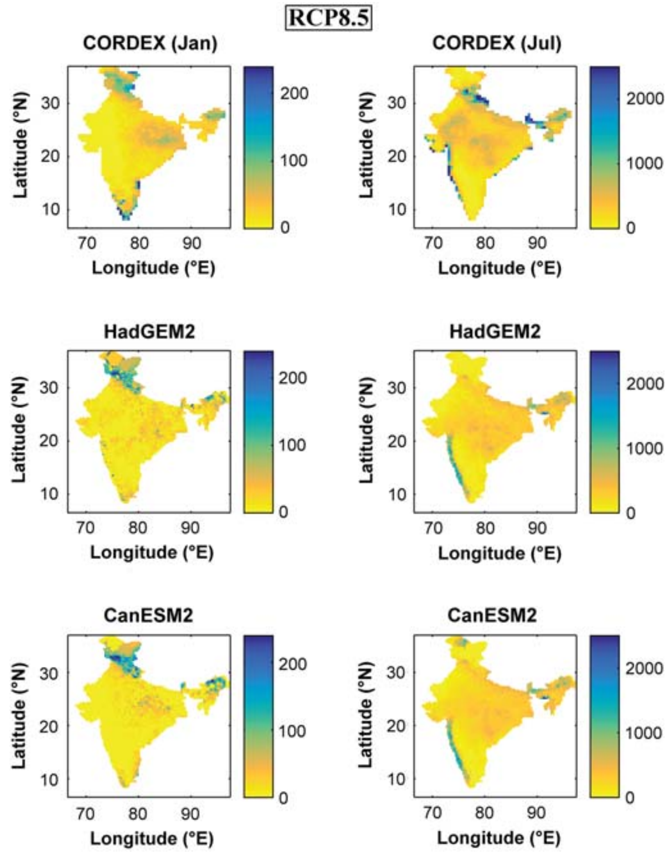

FIGURE 12 Comparison between bias-corrected TVDM (using HadGEM2 and CanESM2) and CORDEX precipitation during future period using RCP8.5 scenario outputs through monthly average precipitation in the January (left panel) and July (right panel) months [Colour figure can be viewed at wileyonlinelibrary.com]

development (1953–1990), model testing (1991–2005) and future period (2006–2035). For demonstration, the results are presented for one non-monsoon month (January) and one monsoon month (July). It is found that the performance of the TVDM downscaled precipitation is matched well with the observed precipitation during the development (Figure 9) and testing periods (Figure 10) whereas the CORDEX precipitation data show a poor match with the observed data during the respective time periods (refer Figures 9 and 10). The outstanding performance of the TVDM in the northern, central, northeast and Western Ghats region is noticed from Figures 9 and 10. The CORDEX data correspond poorly with the observed data in the Western Ghats region. It is worth mentioning that the CORDEX data underestimates the precipitation in the northeast and Western Ghats regions during the July (monsoon) month. It is found to be consistent using the multiple GCMs, viz. HadCM3, HadGEM2 and CanESM2 except in the northern part, where HadGEM2 and CanESM2 slightly overestimate as compared to the HadCM3.

Furthermore, the TVDM is utilized to downscale the precipitation during future period (2006–2035) using the RCP4.5 and RCP8.5 (except HadCM3) scenario outputs obtained from all the three GCMs. The TVDM-downscaled future precipitation for India, along with CORDEX data, are presented in Figure 11 for a typical dry month (January) and a high-rainfall monsoon month (July). The TVDM output shows that there will be a slight increase in precipitation during the future period as compared to the historical data in the western and northeast regions of India and it may slightly decrease in the northern India. Apart from this, the high spatial variation at finer resolution in case of TVDM is very clear from the comparison plots (Figure 11). This is found to have better agreement with the observations in the past as compared to the CORDEX output, which is found to be much smoother than that is noticed in the observed record in the past. The RCP8.5 scenario outputs are also used to downscale the future precipitation using TVDM (using HadGEM2 and CanESM2) and comparison was made with CORDEX data (Figure 12). It can be noted that

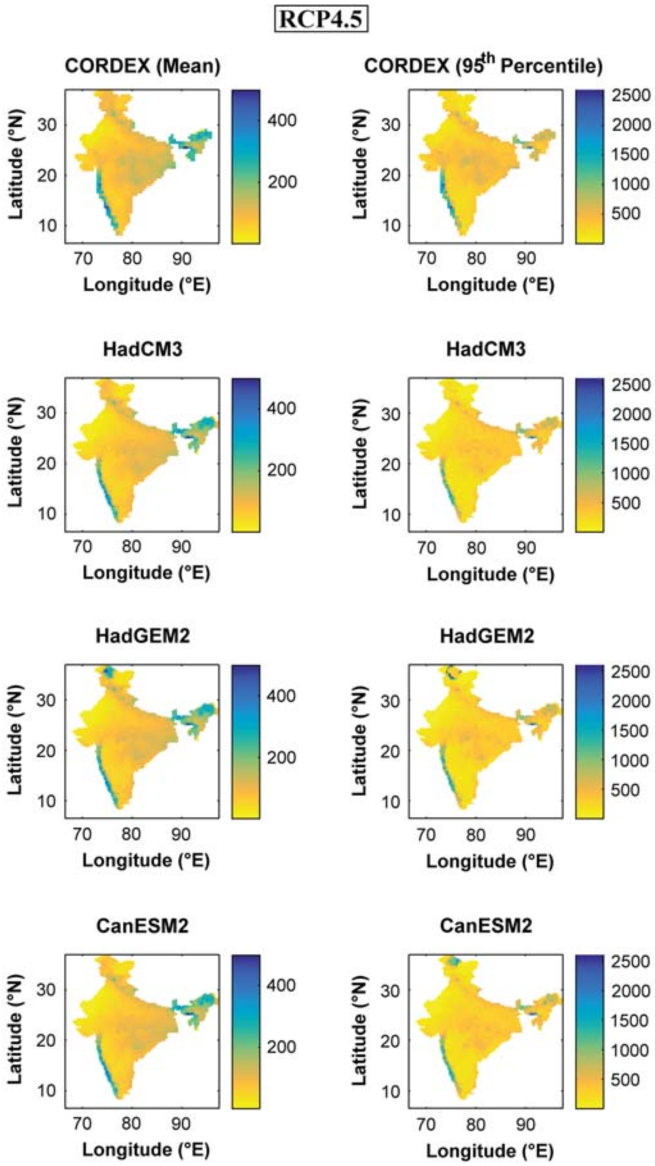

FIGURE 13 Match of mean and 95th percentile values between bias-corrected TVDM downscaled (using HadCM3, HadGEM2 and CanESM2) precipitation and CORDEX (RCP4.5) precipitation during future period (2006–2035) considering CORDEX output as pseudo-observations [Colour figure can be viewed at wileyonlinelibrary.com]

the CORDEX is showing maximum increase in the Himalayan, northeast and Western Ghats regions in the monsoon month (July) and over estimating in the southern part of peninsular India during non-monsoon month (January). The TVDM downscaled precipitation is also implies increase in precipitation in the northeast and Western Ghats regions as compared to historical period (Figure 12). The monthly variation of precipitation based on RCP2.6 scenario is presented in Figure S6. Increase in precipitation is much lower as compared to RCP8.5.

Although RCM output is used in this study as an target to compare the performance of proposed TVDM, it is worthwhile to mentioned that a pseudo-reality approach used RCM outputs as pseudo-observations (Vrac, Stein, Hayhoe, & Liang, 2007). Thus, as an additional study, a pseudo-reality approach is also adopted to check the ability of TVDM in

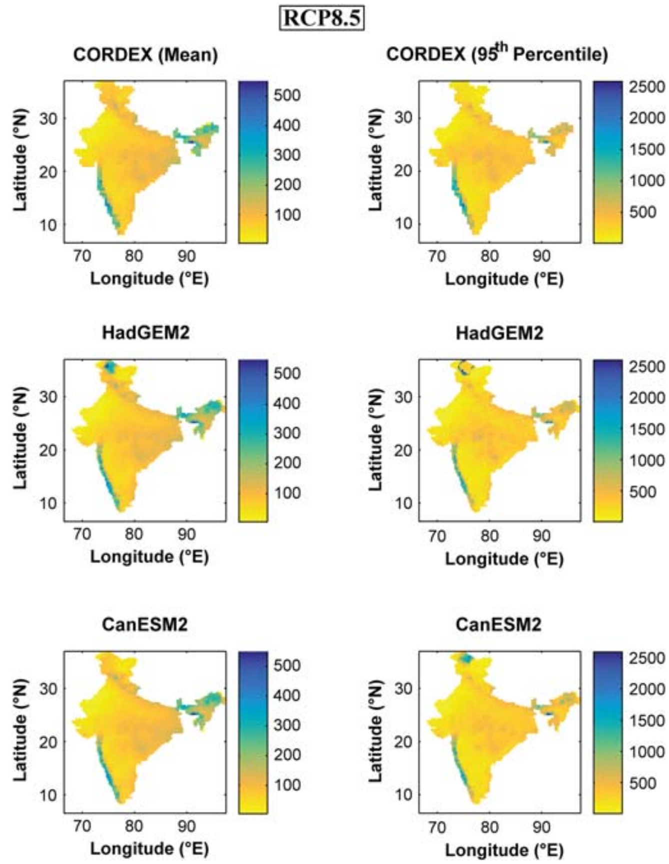

FIGURE 14 Match of mean and 95th percentile values between bias-corrected TVDM downscaled (using HadGEM2 and CanESM2) precipitation and CORDEX (RCP8.5) precipitation during future period (2006–2035) considering CORDEX output as pseudo-observations [Colour figure can be viewed at wileyonlinelibrary.com]

downscaling the future precipitation using RCM outputs as pseudo-observations during the future period. The mean and 95th percentile values during the future period are calculated and compared with the CORDEX RCP4.5 and RCP8.5 outputs. The consistency of results obtained from TVDM outputs is checked by analysing outputs from multiple GCMs (HadCM3, HadGEM2 and CanESM2). The match between TVDM downscaled, and CORDEX RCP4.5 and RCP8.5 scenario outputs are shown in Figures 13 and 14. It is worth mentioning that the TVDM outputs are matching better with bias-corrected CORDEX data all over the study area. However, it seems to be the TVDM outputs in the Western Ghats and northeast regions do not match with the CORDEX data for both the RCPs, that is, RCP4.5 and RCP8.5 scenario (Figures 13 and 14). However, the CORDEX data were also found not to match with the observed data in these regions during the historical period.

While the existence of non-stationarity in the relationship between causal and target variables is supported by the previous studies (Duan et al., 2012; Merkenschlager et al., 2017; Sachindra & Perera, 2016), applicability of the proposed methodology is tested over a vast area (India) with wide variation of climatological conditions and the results are promising for different type of climatology. In brief, it can be concluded that the TVDM downscaled precipitation is closer to the observed precipitation values. Requirement of sufficient historical data and location-specific calibration might be the limitations of the application of TVDM. However, it is true for almost all the data-driven approach, including SDSM and CORDEX. The important issue is that the consideration of *time-varying* properties of the causal–target variables is found to be important, which is the motivation of TVDM. This characteristic helps to consider the possible fact that the statistical relationship between the causal variables and the target variable may not remain constant over time, which is very likely in a changing climate. Thus, developed TVDM is found to have a promise for its application in many hydrological studies dealing with climate change impact assessment.

6 | CONCLUSIONS

This study develops a downscaling method, named as the TVDM considering the non-stationarity issue in the context of climate change. The proposed TVDM differs from the existing SDSM as it incorporates the *time-varying* relationship between the causal variables and the target variable. The approach is based on the Bayesian updating philosophy that updates its parameter at each time step in order to capture the time-varying dynamics in the causal–target variables relationships.

The performance of the developed TVDM is demonstrated considering the India as study area at a spatial resolution of 0.25° (lat.) × 0.25° (lon.). Its performance is contrasted with the existing SDSM (assumes stationarity inherently) and the dynamically downscaled products from CORDEX.

The performance of TVDM is found to be much better than the SDSM and CORDEX high-resolution downscaled data. The time-varying relationship in TVDM is found to offer a better performance with respect to the other two downscaling approaches. While comparing with CORDEX data, the TVDM is found to outperform the CORDEX outputs in terms of capturing spatial variability over India.

It is possible to model the stochastic nature of parameter evolution over time. Based on this, the future projection of downscaling is possible through TVDM. Trend, periodicity and autoregressive components are found to capture the temporal evolution of the parameters. Reasonable accuracy is ensured for a 45-year time horizon in future.

TVDM requires parameter initialization. However, the effect of this initial assumption dies down approximately within 18 time steps (one and a half years). In other words, model outputs are free from initial assumptions of parameter set beyond 2 years from the starting of development period. Thus, use of 2-year data as a spin-up period is recommended in while developing TVDM.

Overall, the developed TVDM has shown some potential in its application in a changing climate due to its time-varying characteristics considering the non-stationarity issue that exists in the relationship between the causal–target variables. In the context of projections driven by greenhouse gas emission/concentration scenarios, multi-model ensembles are recommended to use as large-scale input to TVDM. The ability of TVDM in downscaling the other hydroclimatic variables, such as temperature and evapotranspiration, is kept as future scope of this study.

ACKNOWLEDGEMENTS

This work was partially supported by the Department of Science and Technology, Climate Change Programme (SPLICE), Government of India (Ref. No. DST/CCP/CoE/79/2017(G)) through sponsored projects awarded to the corresponding author. All the data sets used are available in the public domain. URLs are as follows: https://iridl.ldeo.columbia.edu/SOURCES/.IMD/.RF0p25/, http://www.ipcc-data.org/sim/gcm_monthly/AR5/Reference-Archive.html, http://cccr.tropmet.res.in/home/ftp_data.jsp.

ORCID

Rajib Maity http://orcid.org/0000-0001-5631-9553

REFERENCES

Arora, V. K., Scinocca, J. F., Boer, G. J., Christian, J. R., Denman, K. L., Flato, G. M., … Merryfield, W. J. (2011). Carbon emission limits required to satisfy future representative concentration pathways of greenhouse gases. *Geophysical Research Letters*, *38*, 1–6. https://doi.org/10.1029/2010GL046270

Bellprat, O., Kotlarski, S., Lüthi, D., & Schär, C. (2013). Physical constraints for temperature biases in climate models. *Geophysical Research Letters*, *40*, 4042–4047. https://doi.org/10.1002/grl.50737

Bordoy, R., & Burlando, P. (2014, 2012). Stochastic downscaling of climate model precipitation outputs in orographically complex regions: 2. Downscaling methodology. *Water Resources Research*, *50*, 562–579. https://doi.org/10.1002/wrcr.20443

Caesar, J., Palin, E., Liddicoat, S., Lowe, J., Burke, E., Pardaens, A., … Kahana, R. (2013). Response of the HadGEM2 Earth System Model to future greenhouse gas emissions pathways to the year 2300. *Journal of Climate*, *26*(2009), 3275–3284. https://doi.org/10.1175/JCLI-D-12-00577.1

Chen, S.-T., Yu, P.-S., & Tang, Y. H. (2010). Statistical downscaling of daily precipitation using support vector machines and multivariate analysis. *Journal of Hydrology*, *385*, 13–22. https://doi.org/10.1016/j.jhydrol.2010.01.021

Chu, J. T., Xia, J., Xu, C.-Y., & Singh, V. P. (2010). Statistical downscaling of daily mean temperature, pan evaporation and precipitation for climate change scenarios in Haihe River, China. *Theoretical and Applied Climatology*, *99*(1–2), 149–161. https://doi.org/10.1007/s00704-009-0129-6

Duan, J., McIntyre, N., & Onof, C. (2012). Resolving non-stationarity in statistical downscaling of precipitation under climate change scenarios. In *British Hydrological Society Eleventh National Symposium, Hydrology for a changing world*.

Fowler, H. J., Blenkinsop, S., & Tebaldi, C. (2007). Linking climate change modelling to impacts studies: Recent advances in downscaling techniques for hydrological modelling. *International Journal of Climatology*, *27*, 1547–1578. https://doi.org/10.1002/joc.1556

Gabriele, F., & Mannina, G. (2010). Bayesian approach for uncertainty quantification in water quality modelling: The influence of prior distribution. *Journal of Hydrology*, *392*(1–2), 31–39. https://doi.org/10.1016/j.jhydrol.2010.07.043

Ghosh, S., & Mujumdar, P. P. (2008). Statistical downscaling of GCM simulations to streamflow using relevance vector machine. *Advances in Water Resources*, *31*(1), 132–146. https://doi.org/10.1016/j.advwatres.2007.07.005

Giorgi, F., Coppola, E., Solmon, F., Mariotti, L., Sylla, M., Bi, X., … Brankovic, C. (2012). RegCM4: Model description and preliminary tests over multiple CORDEX domains. *Climate Research*, *52*, 7–29. https://doi.org/10.3354/cr01018

Giorgi, F., Gutowski, J., & William, J. (2015). Regional dynamical downscaling and the CORDEX initiative. *Annual Review of Environment and Resources*, *40*(1), 467–490. https://doi.org/10.1146/annurev-environ-102014-021217

Giorgi, F., Jones, C., & Asrar, G. R. (2009). Addressing climate information needs at the regional level: The CORDEX framework. *WMO Bulletin*, *58*, 175–183.

Gordon, C., Cooper, C., Senior, C. A., Banks, H., Gregory, J. M., Johns, T. C., & Wood, R. A. (2000). The simulation of SST, sea ice extents and ocean heat transports in a version of the Hadley Centre coupled model without flux adjustments. *Climate Dynamics*, *16*, 147–168.

He, X., Chaney, N. W., Schleiss, M., & Sheffield, J. (2016). Spatial downscaling of precipitation using adaptable random forests. *Water Resources Research*, *52*, 8217–8237. https://doi.org/10.1002/2016WR019034

Hellström, C., Chen, D., Achberger, C., & Räisänen, J. (2001). Comparison of climate change scenarios for Sweden based on statistical and dynamical downscaling of monthly precipitation. *Climate Research*, *19*(1), 45–55. https://doi.org/10.3354/cr019045

Hertig, E., & Jacobeit, J. (2013). A novel approach to statistical downscaling considering nonstationarities: Application to daily precipitation in the Mediterranean area. *Journal of Geophysical Research: Atmospheres*, *118*, 520–533. https://doi.org/10.1002/jgrd.50112

Hessami, M., Gachon, P., Ouarda, T. B. M. J., & St-Hilaire, A. (2008). Automated regression-based statistical downscaling tool. *Environmental Modelling and Software*, *23*(6), 813–834. https://doi.org/10.1016/j.envsoft.2007.10.004

Hewitson, B. C., & Crane, R. G. (1996). Climate downscaling: Techniques and application. *Climate Research*, *7*, 85–95.

Kannan, S., & Ghosh, S. (2011). Prediction of daily rainfall state in a river basin using statistical downscaling from GCM output. *Stochastic Environmental Research and Risk Assessment*, *25*(4), 457–474. https://doi.org/10.1007/s00477-010-0415-y

Kannan, S., & Ghosh, S. (2013). A nonparametric kernel regression model for downscaling multisite daily precipitation in the Mahanadi basin. *Water Resources Research*, *49*, 1360–1385. https://doi.org/10.1002/wrcr.20118

Laloy, E., Fasbender, D., & Bielders, C. L. (2010). Parameter optimization and uncertainty analysis for plot-scale continuous modeling of runoff using a formal Bayesian approach. *Journal of Hydrology*, *380*(1–2), 82–93. https://doi.org/10.1016/j.jhydrol.2009.10.025

Langousis, A., Mamalakis, A., Deidda, R., & Marrocu, M. (2015). Assessing the relative effectiveness of statistical downscaling and distribution mapping in reproducing rainfall statistics based on climate model results. *Water Resources Research*, *52*, 471–494. https://doi.org/10.1002/2015WR017556

Laprise, R. (2008). Regional climate modelling. *Journal of Computational Physics*, *227*(7), 3641–3666. https://doi.org/10.1016/j.jcp.2006.10.024

Lu, Y., & Qin, X. S. (2014). A coupled K-nearest neighbour and Bayesian neural network model for daily rainfall downscaling. *International Journal of Climatology*, *3236*, 3221–3236. https://doi.org/10.1002/joc.3906

Li, L., Diallo, I., Xu, C., & Stordal, F. (2015). Hydrological projections under climate change in the near future by RegCM4 in Southern Africa using a large-scale hydrological model. *Journal of Hydrology*, *528*(May), 1–16. https://doi.org/10.1016/j.jhydrol.2015.05.028

Maity, R., & Nagesh Kumar, D. (2006). Bayesian dynamic modeling for monthly Indian summer monsoon rainfall using El Niño-Southern Oscillation (ENSO) and equatorial Indian Ocean Oscillation (EQUINOO). *Journal of Geophysical Research*, *111*(D7), D07104. https://doi.org/10.1029/2005JD006539

Manor, A., & Berkovic, S. (2015). Bayesian inference aided analog downscaling for near-surface winds in complex terrain. *Atmospheric Research*, *164–165*, 27–36. https://doi.org/10.1016/j.atmosres.2015.04.014

Maraun, D. (2012). Nonstationarities of regional climate model biases in European seasonal mean temperature and precipitation sums. *Geophysical Research Letters*, *39*, 1–5. https://doi.org/10.1029/2012GL051210

Maraun, D., Widmann, M., Gutiérrez, J. M., Kotlarski, S., Chandler, R. E., Hertig, E., … Wilcke, R. A. I. (2015). VALUE: A framework to validate downscaling approaches for climate change studies. *Earth's Future*, *3*, 1–14. https://doi.org/10.1002/2014EF000259

Merkenschlager, C., Hertig, E., & Jacobeit, J. (2017). Non-stationarities in the relationships of heavy precipitation events in the Mediterranean area and the large-scale circulation in the second half of the 20th century. *Global and Planetary Change*, *151*, 108–121. https://doi.org/10.1016/j.gloplacha.2016.10.009

Mullan, D., Chen, J., & John, X. (2016). Validation of non-stationary precipitation series for site-specific impact assessment: Comparison of two statistical downscaling techniques. *Climate Dynamics*, *46*, 967–986. https://doi.org/10.1007/s00382-015-2626-x

Nagesh Kumar, D., & Maity, R. (2008). Bayesian dynamic modeling for nonstationary hydroclimatic time series forecasting along with uncertainty quantification. *Hydrological Processes*, *22*, 3488–3499. https://doi.org/10.1002/hyp.6951

Nikulin, G., Jones, C., Giorgi, F., Asrar, G., Buchner, M., Cerezo-Mota, R., … Sushma, L. (2012). Precipitation climatology in an ensemble of CORDEX-Africa regional climate simulations. *Journal of Climate*, *25*, 6057–6078. https://doi.org/10.1175/JCLI-D-11-00375.1

Pervez, M. S., & Henebry, G. M. (2014). Projections of the Ganges–Brahmaputra precipitation—Downscaled from GCM predictors. *Journal of Hydrology*, *517*, 120–134. https://doi.org/10.1016/j.jhydrol.2014.05.016

Pichuka, S., & Maity, R. (2016). Spatio-temporal downscaling of projected precipitation in the 21st century: Indication of a wetter monsoon over the Upper Mahanadi Basin, India. *Hydrological Sciences Journal*, *62*(3), 467–482. https://doi.org/10.1080/02626667.2016.1241882

Pope, V. D., Gillani, M. L., Rowntree, P. R., & Strattom, R. A. (2000). The impact of new physical parametrizations in the Hadley Centre climate model: HadAM3. *Climate Dynamics*, *2*, 123–146.

Raje, D., & Mujumdar, P. P. (2009). A conditional random field-based downscaling method for assessment of climate change impact on multisite daily precipitation in the Mahanadi basin. *Water Resources Research*, *45*, 1–20. https://doi.org/10.1029/2008WR007487

Raje, D., & Mujumdar, P. P. (2010). Constraining uncertainty in regional hydrologic impacts of climate change: Nonstationarity in downscaling. *Water Resources Research*, *46*, 1–23. https://doi.org/10.1029/2009WR008425

Rajeevan, M., Bhate, J., Kale, J. D., & Lal, B. (2006). High resolution daily gridded rainfall data for the Indian region: Analysis of break and active monsoon spells. *Current Science*, *91*(3), 296–306.

Ramdas, M., Rehana, S., & Mujumdar, P. P. (2012). Assessment of hydrologic impacts of climate change in Tunga–Bhadra River basin, India with HEC-HMS and SDSM. *Hydrological Processes*, *27*, 1572–1589. https://doi.org/10.1002/hyp.9220

Rashid, M., Beecham, S., & Chowdhury, R. K. (2016). Statistical downscaling of rainfall: A non-stationary and multi-resolution approach. *Theoretical and Applied Climatology*, *124*, 919–933. https://doi.org/10.1007/s00704-015-1465-3

Reichler, T., & Kim, J. (2008). How well do coupled models simulate Today's climate? *Bulletin of the American Meteorological Society*, *89*(3), 303–311. https://doi.org/10.1175/BAMS-89-3-303

Rotach, M. W., Marinucci, M. R., Wild, M., Tschuck, P., Ohmura, A., & Beniston, M. (1997). Nested regional simulation of climate change over the Alps for the scenario of a doubled greenhouse forcing. *Theoretical and Applied Climatology*, *57*(3–4), 209–227. https://doi.org/10.1007/BF00863614

Sachindra, D. A., Huang, F., Barton, A., & Perera, B. J. C. (2014). Statistical downscaling of general circulation model outputs to precipitation—Part 1: Calibration and validation. *International Journal of Climatology*, *34*, 3264–3281. https://doi.org/10.1002/joc.3914

Sachindra, D. A., & Perera, B. J. C. (2016). Statistical downscaling of general circulation model outputs to precipitation accounting for non-stationarities in predictor–predictand relationships. *PLOS one*, *11*, 1–21. https://doi.org/10.1371/journal.pone.0168701

Sarhadi, A., Burn, D. H., Ausin, M. C., & Wiper, M. P. (2016). Time-varying nonstationary multivariate risk analysis using a dynamic Bayesian copula. *Water Resources Research*, *52*, 2327–2349. https://doi.org/10.1002/2015WR018525

Schmidli, J., Goodess, C. M., Frei, C., Haylock, M. R., Hundecha, Y., Ribalaygua, J., & Schmith, T. (2007). Statistical and dynamical downscaling of precipitation: An evaluation and comparison of scenarios for the European Alps. *Journal of Geophysical Research*, *112*, 1–6.

Schnorbus, M., Werner, A., & Bennett, K. (2014). Impacts of climate change in three hydrologic regimes in British Columbia, Canada. *Hydrological Processes*, *28*(3), 1170–1189. https://doi.org/10.1002/hyp.9661

Shepard, D. (1968). A two-dimensional interpolation function for irregularly-spaced data. *In Proceedings of the 23rd ACM National Conference*, pp. 517–524. https://doi.org/10.1145/800186.810616

Singh, C. V. (2006). Pattern characteristics of Indian monsoon rainfall using principal component analysis (PCA). *Atmospheric Research*, *79*, 317–326. https://doi.org/10.1016/j.atmosres.2005.05.006

Stott, P. A., Tett, S. F. B., Jones, G. S., & Allen, M. R. (2000). External control of 20th century temperature by natural and anthropogenic forcings. *Science*, *290*, 2133–2137.

Teutschbein, C., Wetterhall, F., & Seibert, J. (2011). Evaluation of different downscaling techniques for hydrological climate-change impact studies at the catchment scale. *Climate Dynamics*, *37*(9–10), 2087–2105. https://doi.org/10.1007/s00382-010-0979-8

Tisseuil, C., Vrac, M., Lek, S., & Wade, A. J. (2010). Statistical downscaling of river flows. *Journal of Hydrology*, *385*(1–4), 279–291. https://doi.org/10.1016/j.jhydrol.2010.02.030

Tyralis, H., & Koutsoyiannis, D. (2014). A Bayesian statistical model for deriving the predictive distribution of hydroclimatic variables. *Climate Dynamics*, *42*(11–12), 2867–2883. https://doi.org/10.1007/s00382-013-1804-y

Vrac, M., Stein, M. L., Hayhoe, K., & Liang, X. (2007). A general method for validating statistical downscaling methods under future climate change. *Geophysical Research Letters*, *34*, 1–5. https://doi.org/10.1029/2007GL030295

Vrugt, J. A., Braak, C. J. F., Gupta, H. V., & Robinson, B. A. (2009). Equifinality of formal (DREAM) and informal (GLUE) Bayesian approaches in hydrologic modeling? *Stochastic Environmental Research and Risk Assessment*, *23*, 1011–1026. https://doi.org/10.1007/s00477-008-0274-y

West, M., & Harrison, P. J. (1997). *Bayesian forecasting and dynamic models*. New York, NY: Springer.

Wilby, R. L., & Dawson, C. W. (2013). The statistical downscaling model: Insights from one decade of application. *International Journal of Climatology*, *33*(7), 1707–1719. https://doi.org/10.1002/joc.3544

Wilby, R. L., Dawson, C. W., & Barrow, E. M. (2002). SDSM—A decision support tool for the assessment of regional climate change impacts. *Environmental Modelling & Software*, *17*(2), 145–157. https://doi.org/10.1016/S1364-8152(01)00060-3

Wilby, R. L., Hay, L. E., Gutowski, W. J., Arritt, R. W., Takle, E. S., Pan, Z., … Clark, M. P. (2000). Hydrological responses to dynamically and statistically downscaled climate model output. *Geophysical Research Letters*, *27*(8), 1199–1202.

Wilcke, R. A. I., & Lars, B. (2016). Selecting regional climate scenarios for impact modelling studies. *Environmental Modelling & Software*, *78*, 191–201. https://doi.org/10.1016/j.envsoft.2016.01.002

Xue, Y., Janjic, Z., Dudhia, J., Vasic, R., & De Sales, F. (2014). A review on regional dynamical downscaling in intraseasonal to seasonal simulation/prediction and major factors that affect downscaling ability. *Atmospheric Research*, *147–148*, 68–85. https://doi.org/10.1016/j.atmosres.2014.05.001

Yang, J., Reichert, P., Abbaspour, K. C., & Yang, H. (2007). Hydrological modelling of the Chaohe basin in China: Statistical model formulation and Bayesian inference. *Journal of Hydrology*, *340*, 167–182. https://doi.org/10.1016/j.jhydrol.2007.04.006

Zhang, X., & Yan, X. (2015). A new statistical precipitation downscaling method with Bayesian model averaging: A case study in China. *Climate Dynamics*, *45*, 2541–2555. https://doi.org/10.1007/s00382-015-2491-7

SUPPORTING INFORMATION

Additional Supporting Information may be found online in the supporting information tab for this article.

How to cite this article: Pichuka S, Maity R. Development of a time-varying downscaling model considering non-stationarity using a Bayesian approach. *Int. J. Climatol*. 2018;1–20. https://doi.org/10.1002/joc.5491